JAERI-Tech
2003-058

NUCLEAR, THERMO-MECHANICAL AND TRITIUM RELEASE ANALYSIS OF ITER BREEDING BLANKET

June 2003

Yasuo KOSAKU, Toshimasa KURODA, Mikio ENOEDA
Toshihisa HATANO, Satoshi SATO, Sinichi SATOH*
Toshio OSAKI*, Nobuharu MIKI and Masato AKIBA

日本原子力研究所
Japan Atomic Energy Research Institute

本レポートは，日本原子力研究所が不定期に公刊している研究報告書です。
入手の問合わせは，日本原子力研究所研究情報部研究情報課（〒319-1195　茨城県那珂郡東海村）あて，お申し越しください。なお，このほかに財団法人原子力弘済会資料センター（〒319-1195　茨城県那珂郡東海村日本原子力研究所内）で複写による実費頒布をおこなっております。

This report is issued irregularly.
Inquiries about availability of the reports should be addressed to Research Information Division, Department of Intellectual Resources, Japan Atomic Energy Research Institute, Tokai-mura, Naka-gun, Ibaraki-ken, 319-1195, Japan.

編集兼発行　　日本原子力研究所

Nuclear, Thermo-mechanical and Tritium Release Analysis of ITER Breeding Blanket

Yasuo KOSAKU, Toshimasa KURODA, Mikio ENOEDA, Toshihisa HATANO, Satoshi SATO, Sinichi SATOH*, Toshio OSAKI*, Nobuharu MIKI and Masato AKIBA

Department of Fusion Engineering Research
Naka Fusion Research Establishment
Japan Atomic Energy Research Institute
Naka-machi, Naka-gun, Ibaraki-ken

(Received April 24, 2003)

The design of the breeding blanket in ITER applies pebble bed breeder in tube (BIT) surrounded by multiplier pebble bed. It is assumed to use the same module support mechanism and coolant manifolds and coolant system as the shielding blankets. This work focuses on the verification of the design of the breeding blanket, from the viewpoints which is especially unique to the pebble bed type breeding blanket, such as, tritium breeding performance, tritium inventory and release behavior and thermo-mechanical performance of the ITER breeding blanket.

With respect to the neutronics analysis, the detailed analyses of the distribution of the nuclear heating rate and TBR have been performed in 2D model using MCNP to clarify the input data for the tritium inventory and release rate analyses and thermo-mechanical analyses.

With respect to the tritium inventory and release behavior analysis, the parametric analyses for selection of purge gas flow rate were carried out from the view point of pressure drop and the tritium inventory/release performance for Li_2TiO_3 breeder. The analysis result concluded that purge gas flow rate can be set to conventional flow rate setting (88 l/min per module) to 1/10 of that to save the purge gas flow and minimize the size of purge gas pipe. However, it is necessary to note that more tritium is transformed to HTO (chemical form of water) in case of Li_2TiO_3 compared to other breeder materials.

With respect to the thermo-mechanical analyses of the pebble bed blanket structure, the analyses have been performed by ABAQUS with 2D model derived from one of eight facets of a blanket module, based on the reference design. Analyses were performed to identify the temperature distribution incorporating the pebble bed mechanical simulation and influence of mechanical behavior to the thermal behavior. The result showed that the maximum temperature in the breeding material was 617 °C in the first row of breeding rods and the minimum temperature was 328 °C in the seventh row of breeding rods. The temperature range in the Be pebble bed region ranges between 141°C and 503°C. The temperature ranges of breeder and multiplier pebble beds were certified to be acceptable from the view points of material and functional soundness.

In conclusion, the analyses performed in this study showed the justification and possible improvement on the design of the ITER breeding blanket, from the view points of tritium breeding performance, tritium release performance and thermo-mechanical performance.

Keywords: Breeding Blanket, ITER, Pebble Bed, Breeder in Tube, Tritium Breeding Performance, Tritium Inventory, Tritium Release, Thermo-mechanical Performance

---

* Kawasaki Heavy Industries, Ltd.

ITER 増殖ブランケットの核、熱機械、トリチウム放出特性解析

日本原子力研究所那珂研究所核融合工学部
古作 泰雄・黒田 敏公・榎枝 幹男・秦野 歳久、
佐藤 聡・佐藤 真一*・大﨑 敏雄*・三木 信晴・秋場 真人

(2003 年 4 月 24 日受理)

ITER の増殖ブランケット設計は、中性子増倍材微小球充填層中にトリチウム増殖材微小球の管状充填層(BIT)をおく構造を採用している。設計は、遮蔽ブランケットと同一のモジュール支持構造と冷却マニフォールドを使用することを仮定したものである。本研究では、微小球充填層型増殖ブランケットに特有の設計課題を含む、トリチウム増殖性能核解析、トリチウム放出挙動解析、ペブル充填層を考慮した熱機械特性解析を実施し、設計の妥当性を評価した。

ブランケットの核熱挙動の解析に関しては、8 ファセットからなる増殖ブランケットモジュールの単位ファセットを 2 次元でモデル化し、MCNP により核発熱率分布と TBR 分布を詳細評価した。これらの評価データは、トリチウムインベントリ・放出挙動の解析と熱機械挙動の解析の最も重要な入力条件として使用した。

トリチウムインベントリ・放出挙動解析に関しては、Li_2TiO_3 微小球を増殖材に使用する場合について、増殖微小球充填層のパージガス圧損とトリチウム放出挙動の観点から、パージガス流量の選定を行った。9～88 *l*/min の間で設定可能であることが明らかになった。ただし、Li_2TiO_3 を使用する場合には放出トリチウムの化学系として HTO(水)となる比率が他の増殖材に比べて大きい点を考慮する必要があることが明らかになった。

微小球充填層型の単位セル構造の熱機械挙動に関しては、8 ファセットからなる増殖ブランケットモジュールの 1 ファセットを 2 次元でモデル化し ABAQUS で解析を行った。微小球充填層の熱機械挙動を考慮した解析の結果、増殖材の最高温度は第一壁最近接増殖管内で 617℃となり、最低温度は 7 番目の増殖管内部で 328℃となった。また、ベリリウム微小球充填層の温度は 141～503℃の範囲内で、増殖増倍材ともに、許容温度範囲を満たしていることが明らかになった。

本解析研究の結果、ITER の増殖ブランケット設計の妥当性と、改善の可能性が示された。

那珂研究所：〒311-0193 茨城県那珂郡那珂町向山 801－1
*川崎重工業株式会社

Contents

目次

1. Introduction

Breeding blanket of ITER aims at production of tritium as fuel supplement in the later operation period of ITER, replaced to the shielding blanket modules in outboard region with no design modification to the current ITER design. In a reference design concept, a module of the breeding blanket is divided into 8 facets to reduce eddy current in case of VDEs. Breeding blanket of ITER applies the pebble bed type breeder and multiplier to reduce the thermo-mechanical degradation by cracking concerned to occur in solid block materials. The basic design concept of the breeding blanket of ITER applies pebble bed breeder in tube (BIT) surrounded by multiplier pebble bed. Since the breeding blankets is planned to replaced to the shielding blanket with minimal modification of the interface, it is designed to be compatible to the same module support, coolant manifold connection, electrical strap, and coolant condition as those of the shield blanket. In the case of the breeding blankets, helium purge gas is additionally needed for recovery of tritium. However, the design of helium purge gas manifold has not been performed. This work intend to clarify the flow rate requirement to the helium purge gas. With respect to the structure design, sketches of basic configuration have been already proposed, however, the thermo-mechanical integrity has not been analyzed, yet. This work focuses on the verification of the basic concept of the breeding blanket, from the viewpoints of tritium inventory and release behavior, and thermo-mechanical performance of the ITER breeding blanket. Prior to the above mentioned analyses, a neutronics analysis has been performed to clarify the tritium generation rate and nuclear heating rate, which are indispensable input conditions for the analyses. This analysis work has been performed as a part of the ITER-EDA Design Task (TA No. :N 91 TD 05 FJ, Task ID No. :D461-JA, "Shield Blanket Design II").

2. Evaluation of TBR and Nuclear Heating Rate Distribution by MCNP

2.1 Objectives

In the analyses of tritium inventory control and two-dimensional thermo-mechanical performance, the information of TBR distribution and nuclear heating rate in two-dimension was indispensable. This section clarifies the information on nuclear heating rate and tritium breeding ratio by using Monte Carlo Neutral Particle (MCNP) code with two dimensional model which represents one of eight facets of a breeding blanket module.

2.2 Analysis Condition

(1) Calculation Model

The reference structure of a breeding blanket module is shown in Fig. 2-1[1]. A module consists of 8 facets and a backing plate. The backing plate provides the interface connection with the flexible supports, coolant manifolds and purge gas manifolds. Figure 2-2[1] shows the configuration inside the facet. It consists of two unit cells separate by a cooling panel. Each unit cell consists of 14 breeding tubes which are packed with the breeder pebbles. Unit cells are packed with neutron multiplier pebbles. The calculation model of unit facet is shown in Fig. 2-3. The model was generated to represent half part of unit facet. In the calculation model, Be pebble bed and SS side wall were divided into pieces of 5 - 13 mm dimension. Calculation models of the breeder tubes packed with breeder pebbles are shown in Fig. 2-4 and 2-5. There are two types of breeder tubes which have different diameters. The breeder tubes packed with breeder pebbles were divided into four parts in radial direction and angular direction of the tube, as well as the surrounding Be pebble bed. The boundary conditions are perfect reflection at up side, bottom side, right side and left side. The height is assumed 1 m.

(2) Neutron Source

Figure 2-6 shows the configuration of the neutron source and the location of the facet of the blanket module. Neutron source was assumed to be generated uniformly in a line which is assumed to appear at the center of the plasma. The distance between the neutron source and the Be armor surface is 223 cm. Neutron wall loading is 0.78 MW/m^2, which is given by the design condition of ITER.

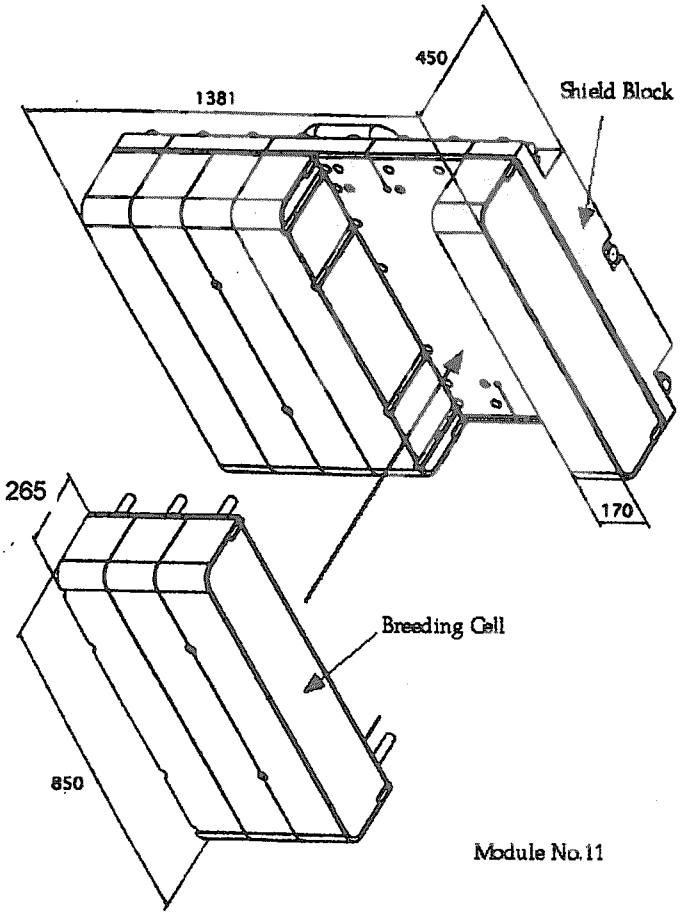

Fig. 2-1 Isometric View of the ITER Breeding Blanket [1]

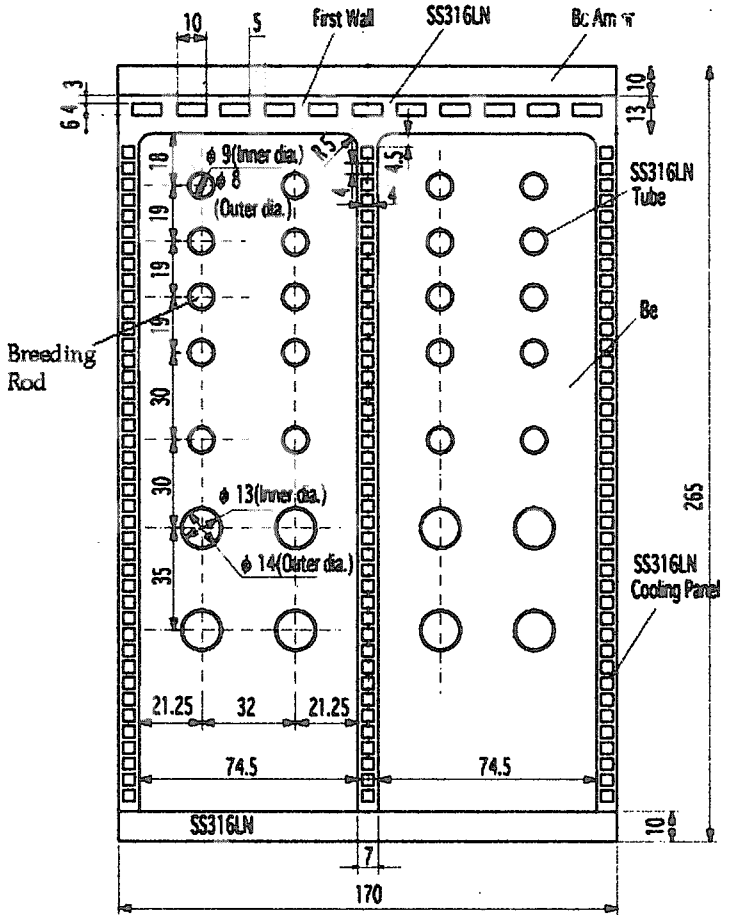

Fig. 2-2 Cross Section of the Breeding Cell of the ITER Breeding Blanket [1]

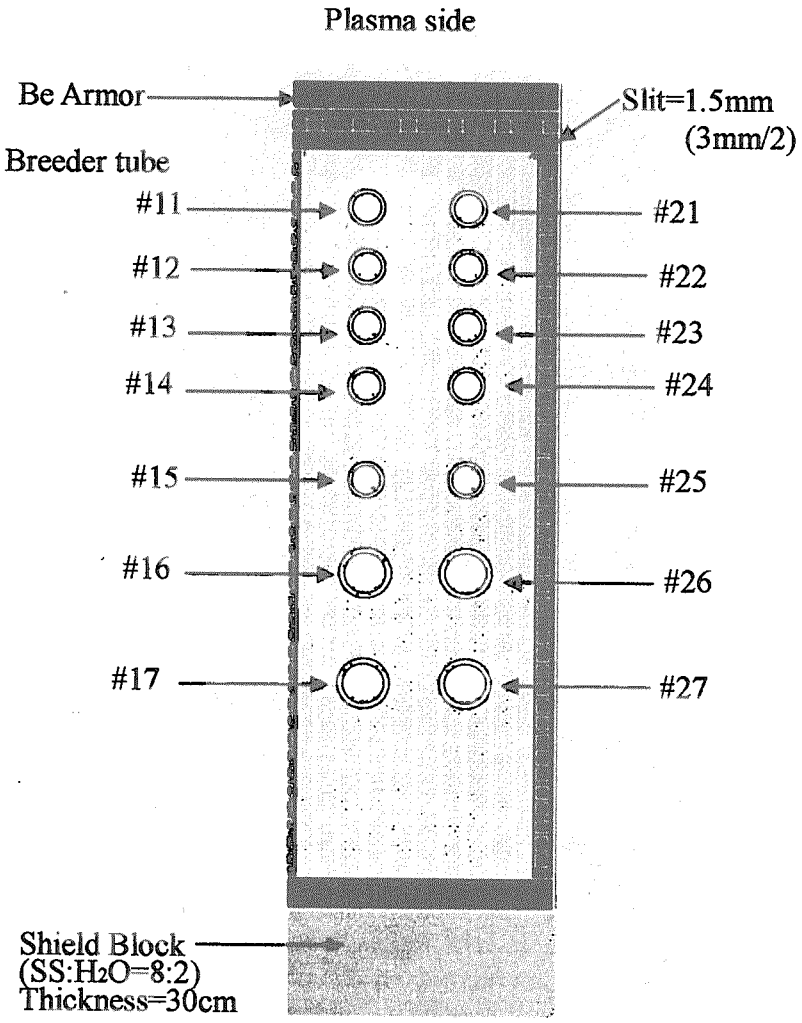

Fig. 2-3 Analysis model of MCNP calculation

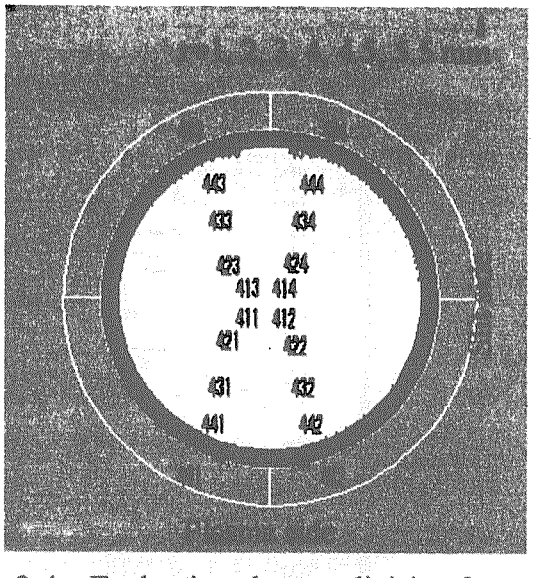

Fig. 2-4 Evaluation element division for breeder tube type 1 (radius = 4 mm)

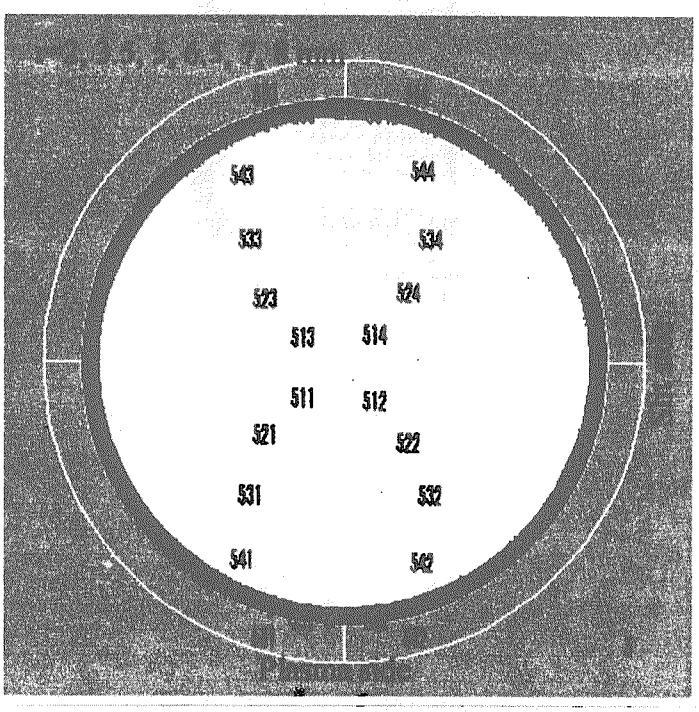

Fig. 2-5 Evaluation element division for breeder tube type 2 (radius = 6.5 mm)

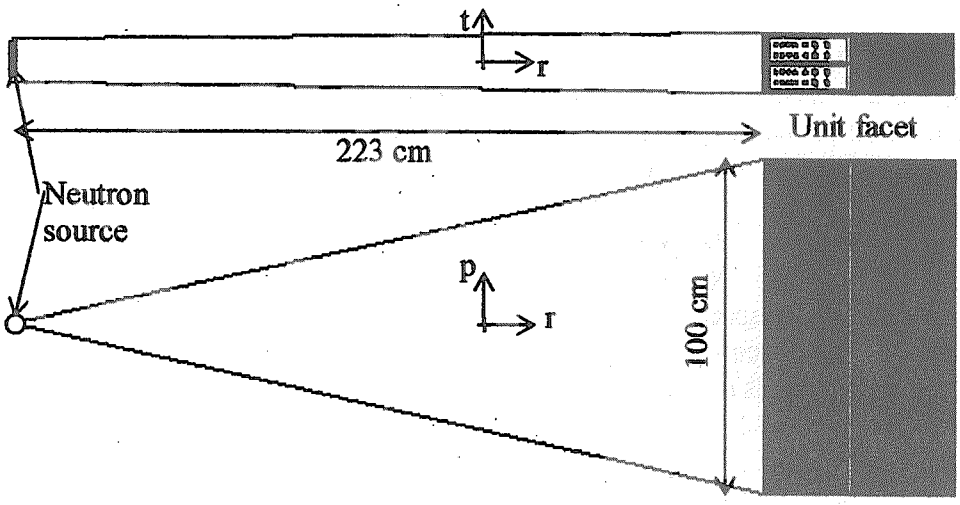

Fig. 2-6 Neutron source setting condition and configuration of the unit facet modeled in this study

2.3 Results

(1) Nuclear Heating Rate

Figure 2-7 shows the distribution of nuclear heating rate of SS, H_2O and Be pebble bed as the function of the thickness of the facet. Material data are as follows.

SS : SS(316L(N)-IG, 0.0858749atom/cm-barn)
H_2O : H_2O (0.9 g/cm^3)
Be : FW armor tiles = 1.85 g/cm^3,
Neutron multiplier pebbles = 100%TD, 63%PF

In Fig. 2-7, black keys represent the nuclear heating rate values of SS tubes of the breeder tubes and Be pebbles near by the breeder tubes. Correlation equations by exponential function for each materials except for Be armor tiles are shown as follows.

SS : $y = 2.24 + 5.85 \times \exp(-(x-2.4)/14.6)$
H_2O : $y = -0.30 + 6.10 \times \exp(-(x-2.95)/19.2)$
Be : $y = 0.08 + 3.03 \times \exp(-(x-2.6)/16.5)$

, where surface of the Be armor tile in plasma side is $x = 0$ cm. The extrapolated value for Be armor by using the correlation above agreed with the calculated value by MCNP within 5 % deviation if the difference of the density was incorporated.

Figure 2-8 shows the calculated value of the breeder pebbles in the breeder tubes. The density of Li_2TiO_3 100%TD is 3.38 g/cm^3. The applied pebble density is 83%TD, 63%PF. Average nuclear heating rate of breeder pebbles in each breeder tubes are 40, 33, 30, 29, 26, 18, 17 MW/m3, at Tube #17(27), #16(26), #15(25), #14(24), #13(23), #12(22), #11(21).

(2) Tritium Breeding Ratio

Table 2-1 shows the summary of the distribution of the tritium breeding ratio (TBR) by tube numbers. TBR values show well averaged distribution by applying larger size of the breeder tube at the rear part of the facet where, neutron attenuation tends to decrease. Total TBR in a facet was estimated 1.003.

Table 2-1 TBR

	^{6}Li	^{7}Li	total
#11	7.872E-02	5.744E-05	7.878E-02
#21	8.178E-02	5.715E-05	8.184E-02
#12	6.549E-02	5.078E-05	6.554E-02
#22	6.894E-02	5.051E-05	6.899E-02
#13	5.850E-02	4.479E-05	5.855E-02
#23	6.265E-02	4.452E-05	6.269E-02
#14	5.646E-02	3.950E-05	5.650E-02
#24	6.020E-02	3.916E-05	6.024E-02
#15	5.112E-02	3.216E-05	5.115E-02
#25	5.453E-02	3.180E-05	5.456E-02
#16	8.990E-02	6.839E-05	8.997E-02
#26	9.603E-02	6.793E-05	9.610E-02
#17	8.668E-02	5.297E-05	8.673E-02
#27	9.122E-02	5.291E-05	9.127E-02
Total			1.003E+00

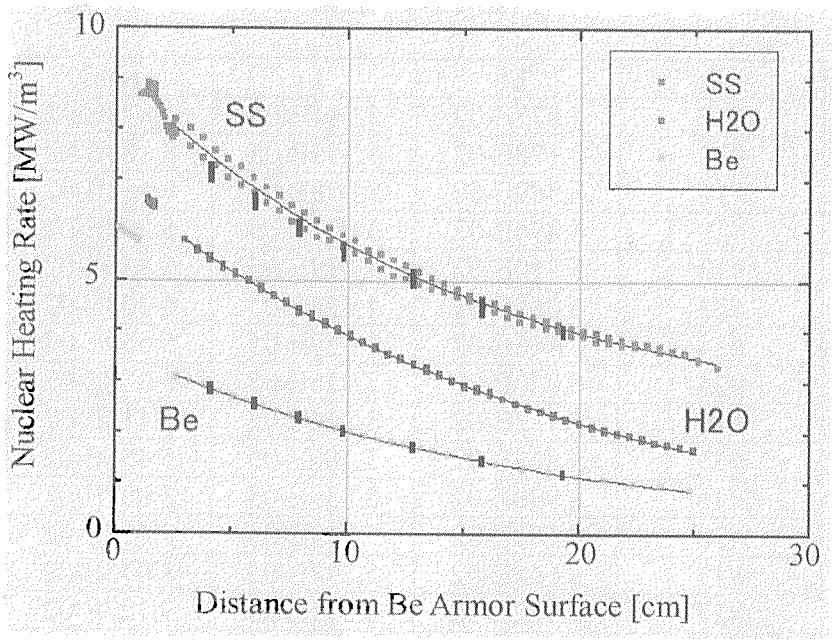

Fig. 2-7 Calculated value of nuclear heating rate of SS, H2O and Be pebble bed

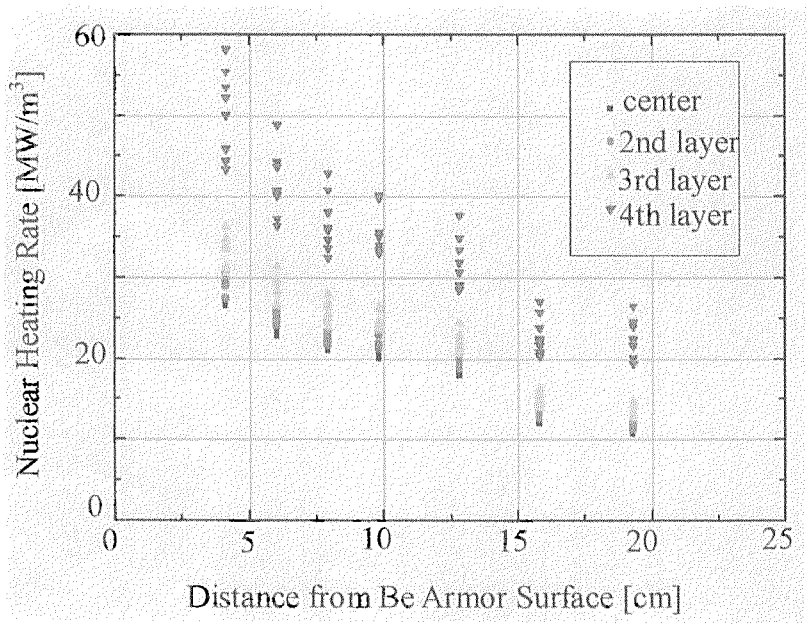

Fig. 2-8 Calculated value of nuclear heating rate in the breeder pebble beds

2.4 Conclusions

By the MCNP calculation, essential information of nuclear heating rates distribution and TBR distribution are clarified, which are the most important design information for the tritium inventory control and thermo-mechanical analysis.

(1) Nuclear heating rate correlation equations are,

SS : $y = 2.24 + 5.85 \times \exp(-(x-2.4)/14.6)$

H_2O : $y = -0.30 + 6.10 \times \exp(-(x-2.95)/19.2)$

Be : $y = 0.08 + 3.03 \times \exp(-(x-2.6)/16.5)$

(2) Average nuclear heating rate of breeder pebbles in each breeder tubes are 40, 33, 30, 29, 26, 18, 17 MW/m^3, at Tube #17(27), #16(26), #15(25), #14(24), #13(23), #12(22), #11(21).

(3) Tritium breeding ratio distribution by the breeder tubes are clarified. Total TBR of a facet was 1.003.

3. Tritium Inventory and Release performance Analyses

3.1 Introduction

Optimization of purge gas flow rate is mainly related to two aspects, pressure drop and tritium inventory and release behavior. Larger flow rate of purge gas results smaller tritium partial pressure in purge gas and smaller inventory, however, causes larger pressure drop of purge gas flow. In case of limited size for purge gas supply tube, quantitative evaluation of purge gas flow rate is necessary from both points of view.

3.2 Analyses Condition

The value of TBR and the temperature change in the breeder tubes are the primary information for optimization of purge gas condition. Figure 2-1 and 2-2 in previous chapter show the schematic structure of the ITER Breeding Blanket for obtaining the necessary information about Tritium Breeding Ratio. Calculation was performed by MCNP by using the calculation model shown in Fig. 2-3 in the previous chapter. Calculated values of TBR are summarized in Table 2-1 in previous chapter. With respect to the temperature distribution in breeder tubes, the major information of temperature distribution from the thermo-mechanical analyses is that temperature range of the breeder tubes are 350 - 600 °C, showing peaking temperature at the center of the tubes (see section 4.3).

3.3 Analyses Procedure

(1) Pressure drop

Pressure drop in a packed bed in lower range of Reynold's number than 10, Kozeny-Carman equation [2] is available as follows.

$$\Delta P = \frac{180(1-\varepsilon)^2}{\varepsilon^3} * \mu u L / d_{pebble}^{\ 2} \quad \text{----------} \quad (3\text{-}1)$$

, where ε is a bed porosity, u is the viscosity[Pa s],u is a superficial gas velocity [m/s], L is the bed length [m], d_{pebble} is the pebble diameter [m]. Viscosity of helium gas is formulated as follows,

$\mu = (3.4351E\text{-}09T^3 - 1.5089E\text{-}05T^2 + 5.2277E\text{-}02T + 5.5421E+00)\times 10^{-6}$ [Pa s] --- (3-2)

, where T is the absolute temperature [K].

Pressure drop in a tube in lower range of Reynold's number than about 4000 can be estimated by laminar flow equation.

$$Re = D_{tube} u \rho / \mu \quad \text{----------} \quad (3\text{-}3)$$

, where Re is the Reynold's number, D_{tube} is a tube diameter [m], u is the velocity [m/s], ρ is the density of the fluid [kg/m^3], μ is the viscosity of the fluid [Pa s].

$$\Delta P = 4f(\rho\mu^2/2)(L/D) \quad \text{----------} \quad (3\text{-}4)$$

, where, L is the tube length [m] and f is Funning's friction factor, which is expressed by the following equation.

$$f = 16/Re \quad \text{----------} \quad (3\text{-}5)$$

(2) Tritium release and inventory

Investigation of tritium release and inventory characteristics in various candidate breeder materials has been performed by many investigators. The investigation clarified that tritium release and inventory characteristics consists of complicated combination of diffusion in solid grain, humidity adsorption on surface, gas-liquid exchange reaction on the grain surface with adsorbed humidity and exchange capacity in solid [3]. Nishikawa et al. integrated many mass transfer steps to the model, by which tritium release behavior can be

calculated as the function of water humidity, H_2 swamping concentration, purge gas velocity and temperature for major candidate breeder pebbles [4].

a) Inventory characteristics

Diffusion [3]

Diffusion in solid grain results the distribution in the grain it self. This distribution is easily integrated and gives the inventory of diffusion.

$$I_D = \frac{G_T d_p^{\,2}}{60 D_T}, \quad D_T = D_0 \exp(\frac{E_D}{RT}) \qquad \text{----------} \qquad (3\text{-}6), (3\text{-}7)$$

I_D: residence time of tritium due to diffusion inventory [s]
G_T : tritium breeding rate [mol/s]
d_p : grain diameter [m]
D_T: diffusion coefficient of tritium in the single crystal of breeder materials [m^2/s]
D_o: pre-exponential factor of diffusion coefficient [m^2/s]
E_D: activation energy of diffusion coefficient [kJ/mol]
R: gas constant [kJ/mol K]
T: absolute temperature [K]

Absorption [3]

In case of Li_2O, LiOH formation and eventual absorption of humidity occur. This phenomenon is peculiar to Li_2O. The temperature dependency is negative.

$$Q_{ab} = Q_{ab0} P_{wat}^{\,n} \exp(\frac{E_{ab}}{RT}) \qquad \text{----------} \qquad (3\text{-}8)$$

Q_{ab}: absorption inventory of tritiated water [mol(water)/mol(breeder)]
Q_{ab0}:Pre-exponential factor of absorption capacity
P_{wat}: partial pressure of water in gas phase [Pa]
E_{ab}: Activation energy of absorption capacity [kJ/mol]

Adsorption [5], [6], [7]

Humidity adsorption on grain surface is the major inventory factor. In case of Li_2TiO_3, 2 different kinds of adsorption were observed.

$$Q_{ad} = Q_{ad0} P_{wat}^{\,m} A \exp(\frac{E_{ad}}{RT}), \quad A = \frac{6}{\rho_s d_p} \qquad \text{--------} \qquad (3\text{-}9), (3\text{-}10)$$

Q_{ad}: adsorption inventory of tritiated water [mol(water)/mol(breeder)]
Q_{ad0}:Pre-exponential factor of adsorption capacity
P_{wat}: partial pressure of water in gas phase [Pa]
E_{ad}: Activation energy of adsorption capacity [kJ/mol]
A: relative surface area of grain [m^2/mol(breeder)]
d_p: grain diameter [m]
ρ_s: breeder material density [mol/m^3]

Exchange capacity [4], [8], [9], [10]

In case of $LiAlO_2$, there detected exchange reaction in high temperature, where humidity adsorption is negligible.

$$Q_{ex} = \frac{Q_{exA} A \exp(\frac{E_{exA}}{RT})}{1 + Q_{exB} \exp(\frac{E_{exB}}{RT})} \quad \text{----------(3-11)}$$

Q_{ex}: exchange reaction inventory of breeder material [mol(tritium)/mol(breeder)]
Q_{exA} , Q_{exB} :Pre-exponential factor of exchange capacity
E_{exA} , E_{exB} : Activation energy of exchange capacity [kJ/mol]
A: relative surface area of grain [m^2/mol]

Isotope exchange between gas phase and adsorption phase [8], [9], [10]
Isotope exchange between gas phase and adsorption phase is assumed to be expressed by the following equations.
H_2(gas) + T_2O(solid) = T_2(gas) + H_2O(solid) ---------- (3-12)
H_2O(gas) + T_2O(solid) = T_2O(gas) + H_2O(solid) ---------- (3-13)
In the exchange reactions (3-12) and (3-13), concentrations of H_2(gas), T_2(gas), H_2O(gas) and T_2O(gas) are calculated as half values of H atoms and T atoms of hydrogen molecules and water molecules in gas phase. Reaction rate coefficients have been determined by the experiments as follows.

$$k_{Fex1} = k_{Fex1,0} \exp(\frac{E_{ex1}}{RT}) \ , \ k_{Fex2} = 2.2 \times 10^{-4} \quad \text{[m/s]} \quad \text{----------(3-14), (3-15)}$$

$$k_{Fex1} \le k_{Fex2} : \quad \alpha_{ex} = \frac{k_{Fex2}}{k_{Fex1}} \ , \ \alpha_{ex}^{'} = 1 \quad \text{----------(3-16), (3-17)}$$

$$k_{Fex1} > k_{Fex2} : \quad \alpha_{ex} = 1 \ , \ \alpha_{ex}^{'} = \frac{k_{Fex1}}{k_{Fex2}} \quad \text{----------(3-18), (3-19)}$$

α : equivalent distribution factor defined by Eqs. (3-16) - (3-19). [-]
k_{Fex1} : apparent exchange reaction rate constant for reaction defined by Eq. (3-12). [m/s]
k_{Fex2} : apparent exchange reaction rate constant for reaction defined by Eq. (3-13). [m/s]

In case of absorption, exchange reaction by gas phase H_2 molecule is negligible. Thus, α_{ex} is infinite and $\alpha_{ex}' = 1$ and Tritium inventory is expressed by

$$Q_{ab,T} = Q_{ab} \frac{P_{T2O}}{P_{Total}} \quad \text{----------(3-20)}$$

$Q_{ab,T}$: tritium inventory by absorption. [mol(tritium)/mol(breeder)]
P_{T2O} : partial pressure of T_2O in gas phase. [Pa]
P_{Total} : total partial pressure of water in gas phase. [Pa]

Tritium inventory by adsorption is expressed by

$$Q_{ad,T} = Q_{ad} \frac{P_{T2O}}{\frac{P_{H2}}{\alpha_{ex}} + \frac{P_{Total}}{\alpha_{ex}^{'}}} \quad \text{----------(3-21)}$$

$Q_{ad,T}$: tritium inventory by adsorption. [mol(tritium)/mol(breeder)]
P_{H2} : partial pressure of H_2 in gas phase. [Pa]

Exchange capacity inventory is expressed by

$$Q_{ex,T} = Q_{ex} \frac{P_{T2O}}{\frac{P_{H2}}{\alpha_{ex}} + \frac{P_{Total}}{\alpha_{ex}'}} \quad \text{----------(3-22)}$$

$Q_{ex,T}$: tritium inventory by exchange reaction. [mol(tritium)/mol(breeder)]

Thus, total inventory is summed up as

$$Q_{Total} = Q_D + Q_{ab,T} + Q_{ad,T} + Q_{ex,T} \quad \text{----------} \quad (3\text{-}23)$$

Q_{Total} : total tritium inventor. [mol(tritium)/mol(breeder)]

Conventionaly, tritium inventory was transformed to the residence time which is the ratio of Tritium inventory and the tritium production rate in each irradiation test.

$$I_{Total} = \frac{Q_{Total}}{G_T} = \frac{Q_D + Q_{ab,T} + Q_{ad,T} + Q_{ex,T}}{G_T} \quad \text{---------} \quad (3\text{-}24)$$

I_{Total} : total tritium residence time. [s]

b) Transient tritium release [4], [11]

Microscopic expression is derived by the surface reaction rate expression as follows.

$$u\frac{\partial P_{H2}}{\partial x} = -k_{F,ex1} a_v X_1 \quad \text{----------(3-25)}$$

$$u\frac{\partial P_{T2}}{\partial x} = k_{F,ex1} a_v X_1 \quad \text{----------(3-26)}$$

$$\rho\frac{\partial Q_H}{\partial t} = -k_{F,ad} X_3 - k_{F,ex2} a_v X_2 \quad \text{----------} \quad (3\text{-}27)$$

$$\rho\frac{\partial Q_T}{\partial t} = -k_{F,ad} X_4 + k_{F,ex2} a_v X_2 \quad \text{----------} \quad (3\text{-}28)$$

$$X_1 = P_{T2} - \frac{(P_{H2}/K + P_{T2})Q_T}{Q_H + Q_T} \quad \text{----------(3-29)}$$

$$X_2 = P_{T2O} - \frac{(P_{H2O} + P_{T2O})Q_T}{Q_H + Q_T} \quad \text{----------(3-30)}$$

$$X_3 = P_{H2O} - P_{H2O}^* \quad \text{----------(3-31)}$$

$$X_4 = P_{T2O} - P_{T2O}^* \quad \text{----------(3-31)}$$

$$Q_H = Q_{H,ad} + Q_{H,abs} + Q_{H,ex} \quad \text{----------} \quad (3\text{-}32)$$

$$Q_T = Q_{T,ad} + Q_{T,abs} + Q_{T,ex} \quad \text{----------} \quad (3\text{-}33)$$

Transient behavior of the pebble bed is calculated by the equation of continuity for the chasing components as following equations.

$$u\frac{\partial P_i}{\partial x} + \rho\frac{\partial Q_i}{\partial t} + \varepsilon\frac{\partial P_i}{\partial t} = 0 \quad \text{----------} \quad (3\text{-}34)$$

P_i : partial pressure of *i* component in gas phase [Pa]
Q_i : holdup of *i* component in breeder pebble [mol(*i*)/mol(breeder)]
t : time [s]
x : location by length from the inlet of the purge gas in flow direction [m]
u: superficial gas velocity [m/s]

ρ : bed packing density [mol(breeder)/m^3]
av : geometrical specific surface area [m^2/m^3]
K : equilibrium constants of hydrogen isotopes of gas to liquid exchange reaction

To tritium release and inventory transient for pebble bed breeder, all equations are to be solved numerically. In this work, the differential equation was derived by implicit differentiation and solved iteratively by improved Eurer method. Table 3-1 summarizes the parameters clarified in references [2] to [14]. Equilibrium constants for gas to liquid exchange reaction of hydrogen isotopes are given by reference [15].

3.4 Analyses Results

(1) Pressure drop

Table 3-2 shows the example of the flow rate plan in case of limiting tritium partial pressure to 1Pa for one facet of the ITER breeding blanket. Total flow rate for one facet is 11 *l*/min and the pressure drop in the breeder tubes (80 cm length, 1mm Li_2TiO_3 pebble 63 % PF) ranged 0.005 to 0.014 MPa. Total purge gas flow rate for one module consists of 8 facets. Figure 3-1 shows the tritium partial pressure and pressure drop in the breeder pebble packed tubes and pressure drop in the purge gas supply pipe, for which dimensions are assumed 5mm inner diameter and 1 m length. Calculation of pressure drops was done by Eqs. (3-1) - (3-5). As can be seen from this figure, conservative purge gas flow rate setting (T_2 partial pressure limitation to 1 Pa) will result pressure drop of 0.014 MPa by breeder tubes and 0.003 MPa by supply pipe. Both pressure drops seem not to cause major purge gas flow problem. In case of setting tritium partial pressure to 10 Pa, pressure drop of each part is almost negligible. Thus, the point of justification is the tritium inventory and the tritium release.

(2) Tritium inventory and release behavior

Figure 3-2 shows the comparison of tritium inventory for major candidate breeder materials as a function of temperature. Calculation was done by Eqs. (3-6) - (3-24). Any breeder material shows relatively small inventory of less than a few hours of residence time in the expected temperature range of 350 - 600 °C. Comparison showed that Li_2TiO_3 has the smallest inventory. Figure 3-4 shows the typical estimation results of tritium release behavior, calculated by Eqs. (3-6) - (3-34). The calculation was done for tube #11 at typical average temperature of 500 °C with purge gas flow rates of 0.4 and 0.865 *l*/min. Temperature transient behavior was assumed to be the same as the FDR breeding blanket, since the basic materials and geometrical configuration is similar. As can be seen from this figure, HTO fraction is larger than HT fraction even though 100 Pa of H_2 is assumed to be added. This is caused by smaller exchange reaction rate as can be seen from the Table 3-1. At the end of 400 sec burn, tritium release seems equilibrated in tube #11. In the rear location of breeder tubes, nuclear heating is relatively small. As can be seen from Fig. 3-3, tritium release behavior depends on temperature change. Thus detailed thermal response should be checked further to examine when the equilibration will be achieved totally. Peaking of HTO release is observed in the estimation. This is caused by the temperature increase. Immediately after burn starts, temperature is still low and generated tritium is stored in the solid phase. By temperature increase, tritium inventory decreases and tritium equilibrium partial pressure increases exponentially, as can be seen from Fig. 3-2. Therefore, if the temperature increase is rapid, discharge rate of tritium from the solid phase increases rapidly. Thus, tritium partial pressure in the gas phase shows the peak and then settle down

to the equilibrium.

Peaking of the HTO release is one of the points to be clarified, because the maximum concentration of tritium is an important design requirement to a tritium recovery system in the down stream. Figure 3-4 shows the peaking partial pressure and time as the function of total flow rate. In case of 8.7 *l*/min total purge gas flow rate, pressure drop is negligibly small, however, HTO peaking will appear at 0.05 hour after plasma burn to 5.5 Pa.

As mention in section 3.2, breeder tube temperature ranges from 350 - 600 °C. Equilibrated HT/HTO fraction is naturally influenced by temperature. Figure 3-5 shows the temperature dependence of the HT/HTO partial pressure in case of 0.86 *l*/min flow rate purge gas with 100 Pa H_2, for typical breeder tube of #11. Incorporating the temperature profile in the radial direction of breeder tube, about 1:1 is estimated for HTO:HT in this case.

HTO:HT ratio is also influenced by H_2 addition. Figure 3-6 shows the effect of H_2 partial pressure at 500 °C, 0.86 *l*/min. As can be seen from this figure, 4000 Pa H2 addition will improve the HTO:HT ratio to about 0.05. Figure 3-7 shows the effect of exchange reaction rate coefficient to HTO:HT ratio in the helium purge gas with the flow rate of 0.86 *l*/min with 100 Pa H_2 addition at 500 °C. In this figure, equivalent values of other breeder material are also marked to show the importance of exchange reaction rate. As can be seen from this figure, high HTO:HT ratio in the case of Li_2TiO_3 is caused by the smaller value of the exchange reaction rate coefficient. In this analysis, the value of exchange reaction coefficient was applied from very small number of experimental data in low temperature (2 experimental points at 100 °C). Further investigation by irradiation test by using fission reactor is waited.

3.5 Conclusions

This analysis is concluded as follows.

(1) Pressure drop of the purge gas is small enough or negligibly small to find space for purge gas tubes in the current ITER design.
(2) Tritium residence time is estimated as small as 0.01 hour, which means tritium release behavior reaches steady state fast.
(3) Chemical form of tritium released in purge gas is estimated 1:1 HTO:HT, which is relatively high HTO fraction compared to other breeder material, because of small value of exchange reaction rate coefficients. Further observation and justification of this value is needed by irradiation test using fission reactors.

Table 3-1 Parameters for major candidate breeder materials by Kyushu University Group
(Values are compiled from references [3] to [14].)

	DT=Do*exp(E/RT) [m^2/s]			Qad1=Qo*Abet*P^n*exp(E/RT) [mol/mol]			Qad2=Qo*Abet*P^n*exp(E/RT) [mol/mol]			Abet [m^2/g]
	Do	E kJ/mol	Ref	Qo	n	E kJ/mol	Qo	n	E kJ/mol	
Li_2O	1.091E-8	-79.47	[11]	8.3E-8	0.75	23.45	---	---	---	0.145
Li_2ZrO_3	1.728E-9	-76.93	[11]	6.3E-6	0.5	10.7	---	---	---	0.145
Li_4SiO_4	2.066E-11	-44.09	[11]	1.2E-6	0.5	13.8	---	---	---	0.145
$LiAlO_2$	2.357E-9	-91.17	[11]	2.6E-7	0.5	32.2	---	---	---	0.145
Li_2TiO_3	1.000E-5	-104	[13]	1.5E-7	0.5	13.4	3.2E-7	0.5	10.6	0.145

	Qab=Qo*P^n*exp(E/RT) [mol/mol]			Qex=A*Abet*exp(Ea/RT)/(1+B*exp(Eb/RT) [mol/mol]			
	Qo	n	E kJ/mol	A	Ea kJ/mol	B	Eb kJ/mol
Li_2O	9.07E-3	0.667	-58.62	---	---	---	---
Li_2ZrO_3	---	---	---	---	---	---	---
Li_4SiO_4	---	---	---	---	---	---	---
$LiAlO_2$	---	---	---	2.7E-15	144	2.2E-12	144
Li_2TiO_3	---	---	---	3.7E-21	174.6	1.1E-16	174.6

(R=8.31451E-03 kJ/molK, av=6/d(pebble))

	Kfex1=Ko*exo(E/RT) [m/s]		Kfex2 [m/s]	Kfad=Ko*exp(E/RT) [m/s]		S dens [g/m^3]	M g
	Ko	E kJ/mol		Ko	E kJ/mol		
Li_2O	8.55E+3	-143	2.2E-4	0.025	-18.26	2.024E+6	29.88125
Li_2ZrO_3	1.6E+2	-121	2.2E-4	0.025	-18.26	4.153E+6	153.0994
Li_4SiO_4	1.84E+3	-134	2.2E-4	0.025	-18.26	2.393E+6	119.8273
$LiAlO_2$	1.84E+3	-134	2.2E-4	0.025	-18.26	2.614E+6	65.92575
Li_2TiO_3	5.0*	-121	2.2E-4	0.025	-18.26	3.435E+6	109.78

*reference [13]

Table 3-2 Conventional purge gas setting by limiting T_2 partial pressure to 1 Pa

Tube #	Tube Radius	T Production rate	Superficial velocity	Volumetric velocity	Pressure Drop
	[cm]	[g-T/s/g-Li2O/min]	SV [cm/s]	V [l/min]	DP [Pa]
#11	0.4	1.5644E-08	28.39	0.8563	1.119E+04
#21	0.4	1.6251E-08	29.50	0.8896	1.163E+04
#12	0.4	1.3014E-08	23.62	0.7124	9.313E+03
#22	0.4	1.3700E-08	24.86	0.7499	9.804E+03
#13	0.4	1.1625E-08	21.10	0.6364	8.319E+03
#23	0.4	1.2449E-08	22.60	0.6815	8.909E+03
#14	0.4	1.1220E-08	20.36	0.6142	8.029E+03
#24	0.4	1.1962E-08	21.71	0.6548	8.560E+03
#15	0.4	1.0158E-08	18.44	0.5560	7.269E+03
#25	0.4	1.0834E-08	19.66	0.5930	7.753E+03
#16	0.4	1.7866E-08	32.43	0.9780	1.279E+04
#26	0.4	1.9083E-08	34.64	1.0446	1.366E+04
#17	0.65	6.5222E-09	11.84	0.9428	4.667E+03
#27	0.65	6.8634E-09	12.46	0.9921	4.911E+03
Total				10.9014	

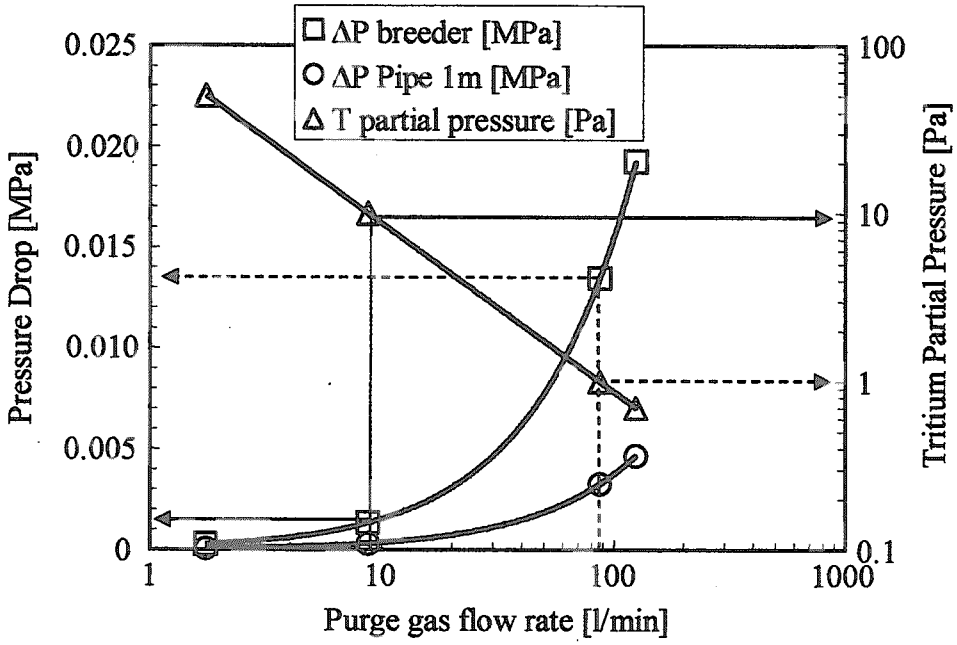

Fig. 3-1 Purge gas flow rate - T partial pressure and DP

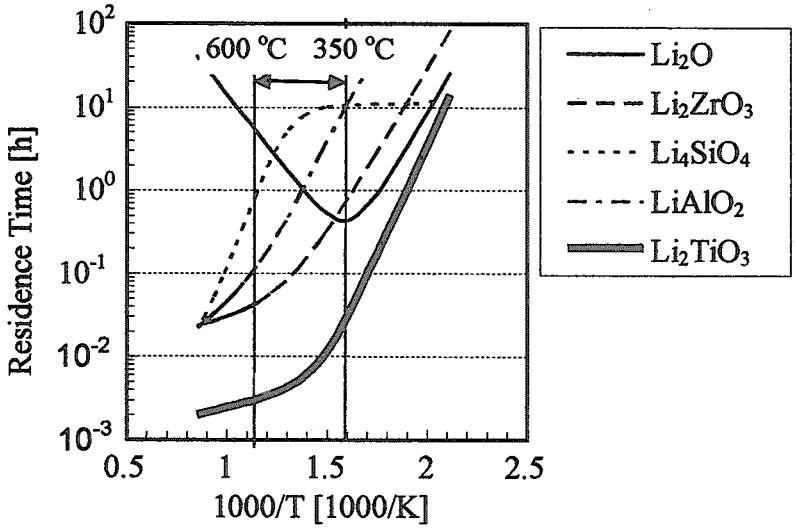

Fig. 3-2 Tritium inventory shown by residence time

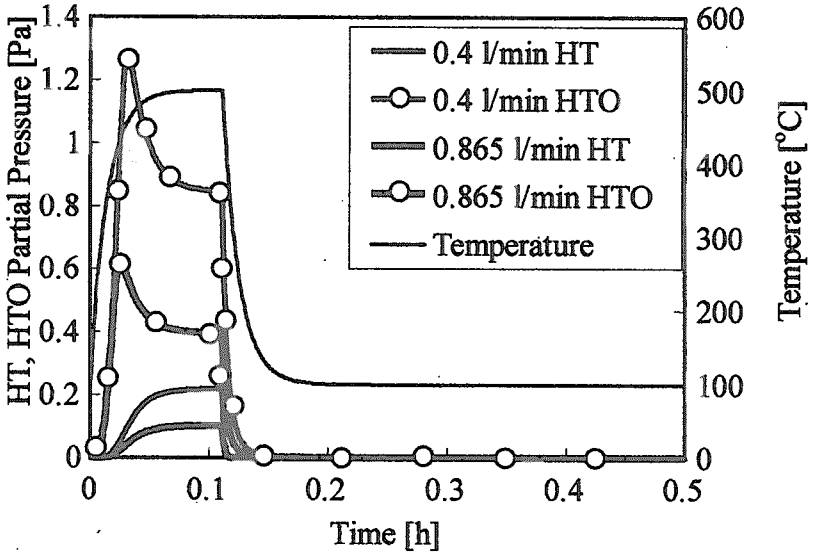

Fig. 3-3 Tritium Release in different purge flow rate

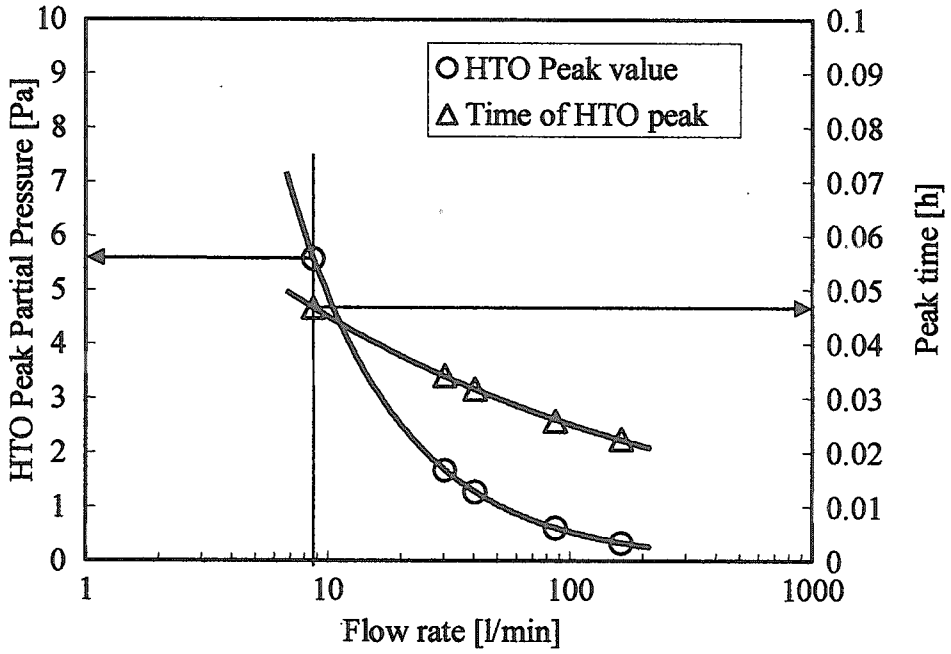

Fig. 3-4 Peak of HTO release after plasma burn

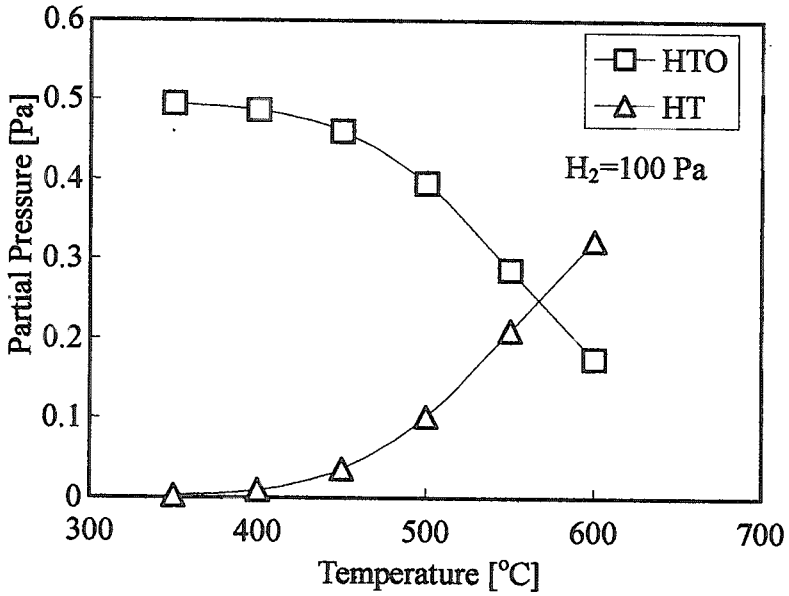

Fig. 3-5 Temperature dependence of HTO and HT partial pressure in steady state

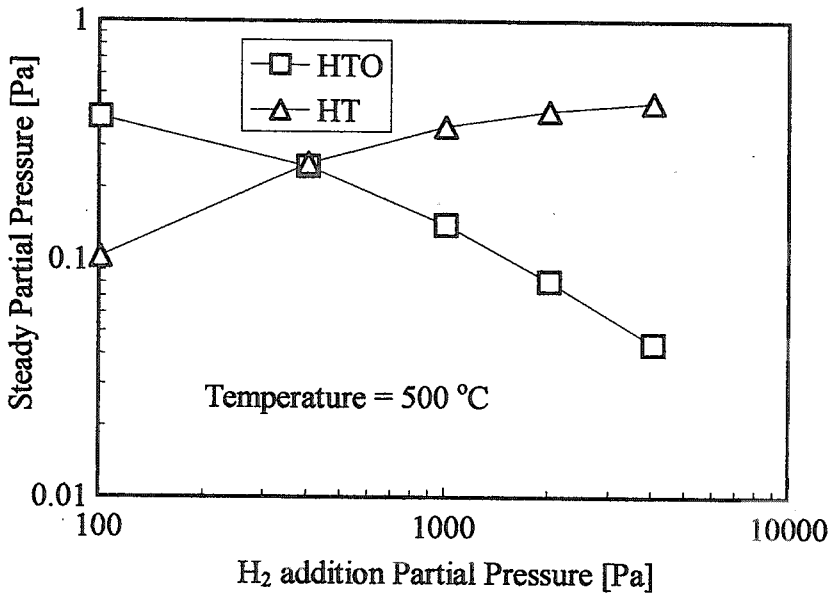

Fig. 3-6 Steady state fraction H2 addition effect

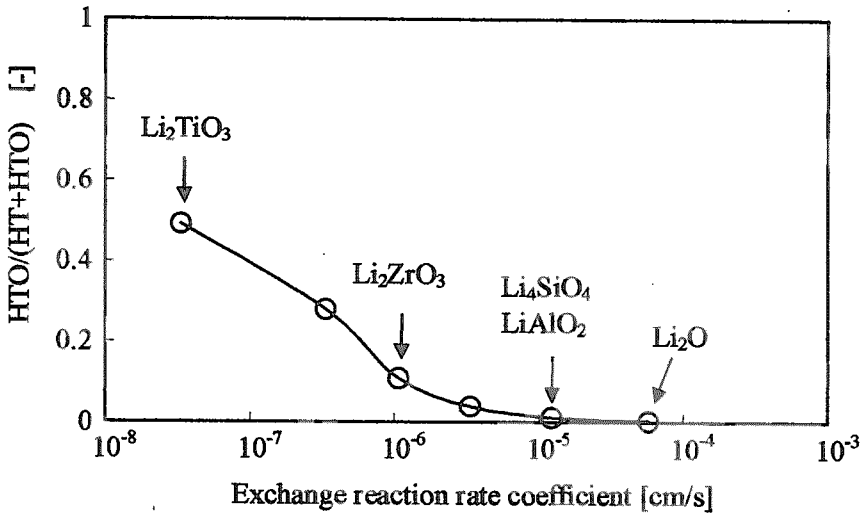

Fig. 3-7 Effect of exchange rate coefficient

4. Thermo-mechanical analysis of the breeding blanket with pebble bed

4.1 Introduction

The design of the breeding blanket of ITER-FEAT, a ceramic-breeder, water-cooled breeding blanket, has been developed to be replace with the outboard shielding blanket in later operation period of ITER. The design is based on modular design similar to the shielding blanket modules. The design concept of the breeding blanket modules have been selected to be compatible with shielding blanket where the attachment method to the vacuum vessel, the maintenance procedure, and the water coolant parameters are the same for both blankets [15]. Figure 4-1 [16] and 4-2 [16] show isometric views of the outboard No.11 breeding blanket. The breeding blanket has ~8 separated breeding cells welded to the shield plate. Total thickness of the breeding blanket is 450mm. The radial thickness of the breeding cell and the shielding plate are ~265mm and ~185mm, respectively.

This chapter clarifies a preliminary thermo-mechanical analysis for the breeding blanket, which have been performed in the case of normal operation at beginning of life. A 2D model of the breeding cell in outboard module No.11 was used to evaluate the temperature and stress distribution in the components.

4.2 Conceptual Design of Breeding Blanket

The breeding blanket module (outboard No.11) has 8 breeding cells embedded in beryllium with three coolant panels used to cool the module. Figure 4-3 shows the isometric views of the breeding cell [16]. The breeding cells are welded to the shield plate at the top and bottom area. The dimension of the breeding cell is ~170mm (toroidal) × ~850mm (poloidal) × ~265mm (radial). The cross section of a breeding cell is shown in Fig. 4-4. In a breeding cell, the breeder rods are arranged in two toroidal rows. Each breeding tube is composed of a type 316LN stainless steel with the breeding materials in the form of pebbles. All the space between the breeding tube and surrounding structure is filled with beryllium neutron multiplier in the form of a single pebble packing bed. The first wall consists of 13 mm thick 316LN stainless steel plate with built-in rectangular coolant channels 4 mm × 10 mm separated by ~ 5 mm walls. A 10mm beryllium is used as armor material to protect the first wall from the plasma interaction. The cooling panels inside the blanket module are similar to the first wall but are only 7mm total thickness and have 4mm × 4mm coolant

channels separated by 1.5 mm thick walls. In this study, lithium titanate (Li_2TiO_3) has been selected for the breeding material.

4.3 Analysis Condition

(1) Analysis Method and Code

The modified Drucker-Prager/Cap plasticity of ABAQUS [17] code is applied to this analysis because this model can treat hydrostatic plastic compression of the pebble bed. As shown in Fig. 4-5, the constitutive equation of the cap model can handle the two yield surfaces expressing the features of pebble bed. In the region bounded by the two yield surfaces the pebble beds show elastic behavior. During the EDA for 98-ITER, a thermo-mechanical analysis for the breeding blanket have been performed by using the modified Drucker-Prager/Cap model [18]. The analysis results using the cap model qualitatively represent well the pebble bed mechanical behavior observed in the experiment, i.e. hydrostatic plastic compression and stress - strain curve due to shear failure [18]. Therefore, the same analytical method and model were applied to this study.

(2) Analysis Model and Conditions

Unit cell of outboard No.11 breeding blanket was provided for this analysis. As shown in Fig. 4-6, 2D toroidal-radial model with plane strain elements was applied to this analysis. The generalized plane strain condition is desirable but unavailable for the coupled temperature-displacement analysis at present [18].

(3) Input data for Analysis

1) Thermal Load

The following thermal load conditions are considered in this analysis.

- Surface heat flux on FW armor : $0.5MW/m^2$
- Radial distribution of nuclear heating in Beryllium : see Fig. 4-7
- Radial distribution of nuclear heating in SS316LN : see Fig. 4-8
- Nuclear heating in breeding material (Li_2TiO_3) : see Fig. 4-9

Nuclear heating distribution in the breeding cell was analyzed by using Monte Carlo transport code. The analysis conditions are as follows.

- Neutron wall load : 0.78 MW/m^2 (outboard mid-plane module)
- Be pebbles : Single size, 100%TD, 63%PF
- Li_2TiO_3 pebbles : Single size, 83%TD, 63%PF

2) Cooling Parameter

Cooling flow in the breeding blanket is shown in Fig. 4-10 [16].

- Coolant : Water, 100°C (Inlet), 3MPa (Inlet)
- Heat transfer coefficient, h
  ; FW Cooling Channel : h = 24970W/m^{2}K
  ; Cooling Plate : h = 10540W/m^{2}K

3) Effective thermal conductivity of Be pebble bed

Effective thermal conductivity of the single size Be pebble bed is calculated from the latest experimental data [19]. Fig. 4-11 shows the relationship between compressive stress and effective thermal conductivity of single size pebble (diameter = 1mm) bed [19]. The present data exhibit a nonlinear dependence between thermal conductivity and compressive stress. The temperature effect is not very remarkable. Therefore, the average line in Fig. 4-11 is applied to the effective thermal conductivity of the Be pebble bed.

4) Effective thermal conductivity of Li_2TiO_3 pebble bed

Effective thermal conductivity in the Li_2TiO_3 pebble bed is estimated with the Schulunder-Zenner-Bauer (SZB) correlation model [20, 21] as shown in Fig. 4-12. The effect of compressive stress is not considered because there are not sufficient data for the dependence between compressive stress and the effective thermal conductivity of the Li_2TiO_3 pebble bed. The calculation conditions for the SZB correlation model are shown as follows.

Calculation Conditions :

Li_2TiO_3 Pebble Bed : Single Size Pebble (Diameter = 1mm)
SZB Correlation Model : Contact Area Fraction = 4.9×10^{-3}
: Accommodation Coefficient = 0.2

5) Heat transfer coefficient at near wall elements

The heat transfer coefficient between Li_2TiO_3 /Be pebble beds and the near wall elements (SS316LN) was not considered in this analysis.

6) Thermal and Mechanical Properties for Be (Armor) and SS316LN

Thermal and Mechanical Properties for Be (Armor) and 316LN stainless steel are shown in Table 4-1.

7) Mechanical Data

Mechanical data for the cap model are summarized in Table 4-2. Another mechanical data for this analysis are shown as follows.

- Young's modulus

The Young's modulus for the beryllium single pebble bed was calculated from experimental data [19]. Figure 4-13 shows the stress-strain dependence measured for a Be pebble bed with 1mm pebbles at ambient temperature [19]. The stress-strain relationship correlation shown bellow is considered for this analysis.

Young's Modulus, E (MPa) = 870*Stress^0.65 (Stress : ~6MPa)

The Young's modulus for Li_2TiO_3 single pebble bed is also calculated from experimental data [22]. Figure 4-14 shows the stress-strain dependence measured for a Li_2TiO_3 pebble bed with 1mm pebbles at ambient temperature [22].

8) Cap Hardening Data

- Be pebble bed

Minimum cap position is assumed to be 1 MPa. Another cap hardening pressure is determined as shown in Table 4-2 based on the inclination of cap hardening line as 1/5 of Young's modulus.

- Li_2TiO_3 pebble bed

Minimum cap position is assumed to be 1 MPa. Another cap hardening pressure is determined as shown in Fig. 4-15 in which 1st loading and 1st unloading lines are drawn based on Fig. 4-14.

$$P = \frac{1}{3}(\sigma_{a1} + 2\sigma_r) = \frac{1}{3}(1 + 2k_0)\sigma_{a1} = 2.5MPa$$

,where P : hydrostatic pressure, MPa

ε_{a1}, ε_{a2} : axial strain (0.0075, 0.005 ; Fig. 4-15)

σ_{a1} : axial stress (4.5MPa ; Fig. 4-15)

ν : Poisson's ratio (0.25)

k_o : $=\sigma_r/\sigma_a$ (0.339 : temporarily assumed to be the same as that for Al pebbles because of no available data for Li_2TiO_3 at present)

$\varepsilon_{vol}^{pl} = \varepsilon_{a2} = 0.005$

Since the inclination of cap hardening line is calculated as 500 MPa (=2.5MPa/0.005), the hydrostatic pressure is 500 MPa atε_{vol}^{pl} =1.

9) Shear Failure Data

The shear failure data for this analysis is summarized in Table 4-2. The friction angle used here is 30.6° for 2D X-Y model with plane strain condition.

4.4 Analysis Results

(1) Temperature Distribution

The steady state temperature distribution in the breeding cell is shown in Fig. 4-16. Also, temperature distributions in the Be pebble bed and breeding material are shown in Fig. 4-17 through Fig. 4-19. The analyzed temperature range in each breeding material (Li_2TiO_3) is shown in Fig. 4-20. The maximum and minimum temperatures in the breeding material (Li_2TiO_3) are summarized for each breeder rod in Table 4-3. The maximum temperature in the breeding material of 617 °C is located in the 1st breeding rod and the minimum temperature is 328 °C in the 7th breeding rod. In case that the lower temperature limit for Li_2TiO_3 pebbles to allow an efficient tritium release is assumed to be 335-380 °C [23], the analyzed minimum temperature, 328 °C, is slightly lower than the limit. However, since the heat transfer coefficient between the breeding rod and breeding material is not considered in this analysis, it is expected that the temperature of the breeding material would slightly become higher. The temperature range in the Be pebble bed region ranges between 141 °C and 503 °C. The analyzed maximum temperature, 503 °C, is almost equal to the maximum temperature limit (~500 °C) to have a sufficient margin with beryllium/steam interaction in accidental

situations. Minor modification of the rod arrangement will be needed to maintain adequate temperature margins for Be and Li_2TiO_3 pebble bed.

(2) Stress Distribution

The stress distributions in the X (radial) and Y (toroidal) direction for the breeding cell are shown in Fig. 4-21 and Fig. 4-22. Also the maximum and minimum stress is summarized in Table 4-4. The stress distributions in the Li_2TiO_3 breeder region are shown in Fig. 4-23 and Fig. 4-24. Tensile stress is found in the most part of the breeding rod because the thermal expansion coefficient of Li_2TiO_3 is smaller than that of the rod wall (type 316LN stainless steel). The stress range in the beryllium multiplier is -6.2MPa~-0.9MPa (X-direction) and -5.8MPa~-1.3MPa (Y-direction) as shown in Fig. 4-25 and Fig. 4-26. High compressive stress is observed in the higher temperature region, so compressive stresses in the region near the breeding rod and far from the cooling panel is higher than the other region. As can be seen from Figs. 4-21 and 4-22, stresses in the stainless steel (FW, cooling panel, breeding rod, back wall) are estimated very high, because the plane-strain condition was applied in this analysis. It is desirable to perform analysis with generalized plane-strain condition or 3D model to obtain more detailed results.

4.5 Summary

A preliminary thermal and stress analysis has been performed for the breeding cell of the blanket module. A Li_2TiO_3 ceramic breeder with beryllium neutron multiplier and water coolant is tentatively used for this study. The analysis results obtained in this study are as follows.

(1) The maximum temperature in the breeding material of 617 °C is located in the 1st breeding tube and the minimum temperature is 328 °C in the 7th breeding tube.

(2) The temperature range in the Be pebble bed region ranges between 141°C and 503°C. The maximum temperature, 503 °C, is almost equal to the maximum temperature limit (~500 °C) of Be.

(3) Minor modification of the rod arrangement will be needed to maintain adequate temperature margins for Be and Li_2TiO_3 pebble bed.

(4) Tensile stress is found in the most part of the breeding tube because the thermal expansion coefficient of Li_2TiO_3 is smaller than that of the breeding tube.

(5) The stress range in the beryllium pebble bed is -6.2MPa~-0.9MPa (radial-direction) and -5.8MPa~-1.3MPa (toroidal-direction).

Table 4-1 Thermal and Mechanical Properties

Beryllium

Temperature (°C)	Thermal Conductivity (W/mK)	Thermal Expansion ($x10^5$/K)	Young's Modulus (GPa)	Poisson's Ratio
20	184.51	1.13	308	0.071
50	176.95	1.19	306	0.07
100	165.30	1.29	304	0.069
150	154.77	1.38	303	0.068
200	145.29	1.47	302	0.067
250	136.77	1.55	300	0.065
300	129.14	1.63	298	0.064
350	122.33	1.70	294	0.063
400	116.26	1.77	288	0.062
450	110.86	1.83	279	0.060
500	106.05	1.88	267	0.059
550	101.75	1.94	251	0.058
600	97.89	1.99	232	0.057
650	94.39	2.03	207	0.055
700	91.17	2.07	176	0.054
800	85.3	2.15	97	0.052

316LN stainless steel

Temperature (°C)	Thermal Conductivity (W/mK)	Thermal Expansion ($x10^5$/K)	Young's Modulus (GPa)	Poisson's Ratio
20	13.94	1.59	192	0.3
50	14.37	1.61	190	0.3
100	15.08	1.64	186	0.3
150	15.80	1.67	182	0.3
200	16.52	1.70	178	0.3
250	17.24	1.72	174	0.3
300	17.95	1.75	170	0.3
350	18.67	1.77	166	0.3
400	19.39	1.79	161	0.3
450	20.10	1.81	157	0.3
500	20.82	1.83	153	0.3
550	21.54	1.85	149	0.3
600	22.26	1.87	145	0.3
650	22.97	1.89	141	0.3
700	23.69	1.91	137	0.3
800	25.12	1.93	129	0.3

Table 4-2 Mechanical Data for Analysis of the Breeding Cell

a) Elastic Constant

	Beryllium Pebble Bed	Li_2TiO_3 Pebble Bed
Young's Modulus	2.8GPa	1.8GPa
Poisson's Ratio	0.25	0.25

b) Shear Failure Data

	Beryllium Pebble Bed	Li_2TiO_3 Pebble Bed
Cohesion, d	0.5MPa	0.5MPa
Friction Angle, β	30.6°	30.6°
Parameter for cap center shift, R	0.5*	0.5*
Initial Plastic Volume Strain, $\varepsilon_{vol}^{pl}(0)$	0**	0**
Parameter for Transition Surface, α	0*	0*
Yield Stress Ratio, K	1*	1*

c) Cap Hardening Data

Beryllium		Li_2TiO_3		Notes
p (MPa)	ε_{vol}^{pl}	p (MPa)	ε_{vol}^{pl}	
1	0	1	0	minimum cap position
56	0.1	50	0.1	-
560	1	500	1	-

* : Typical values are temporarily assumed based on the ABAQUS Standard user's manual.
** : No initial plastic volume strain is assumed.

Table 4-3 Results of Temperature Analysis

Item	Be Armor	Breeder(Li_2TiO_3)							Be Pebble Bed	Structure (SS)
		1st Row	2nd Row	3rd Row	4th Row	5th Row	6th Row	7th Row		FW, Breeding Rod, Cooling Panel, Back Wall
Max. Temp (°C)	283	562	593	588	567	529	617	579	503	503
Min. Temp. (°C)	242	348	409	411	396	375	347	328	141	109

Table 4-4 Results of Stress Analysis

Item		Breeder (Li_2TiO_3)	Be Pebble Bed	Structure (SS) (FW, Breeding Rod, Cooling Panel, Back Wall)
Max. Stress (Pa)	σ_x	4.4E+5	-9.2E+5	1.4E+8
	σ_y	4.6E+5	-1.3E+6	5.9E+8
	σ_{mises}	5.2E+5	2.8E+6	1.3E+9
Min. Stress (Pa)	σ_x	-3.3E+4	-6.2E+6	-8.2E+7
	σ_y	2.4E+5	-5.8E+6	-3.5E+8
	σ_{mises}	3.0E+5	1.0E+6	3.3E+8

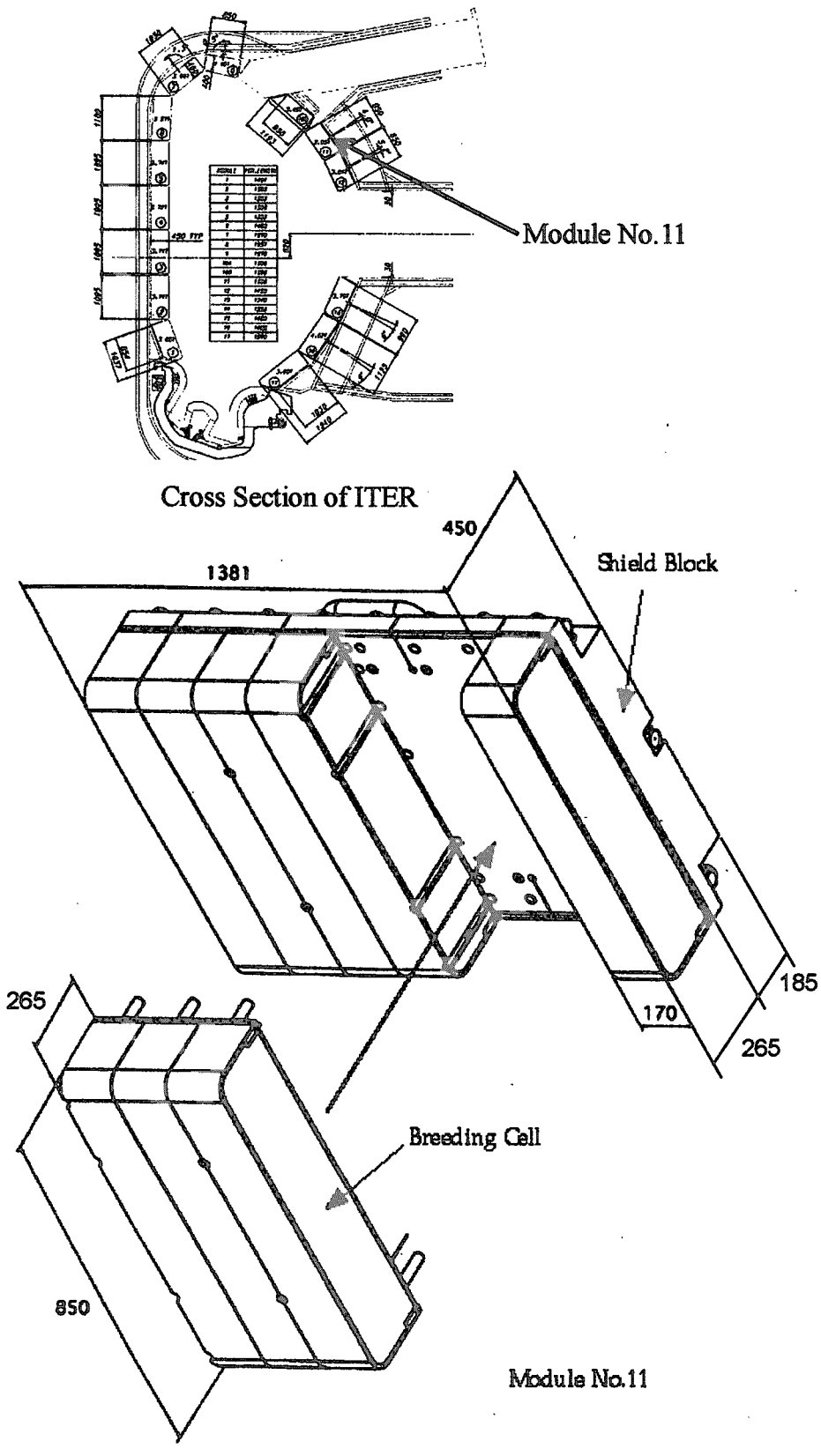

Fig. 4-1 Front View of the ITER Breeding Blanket

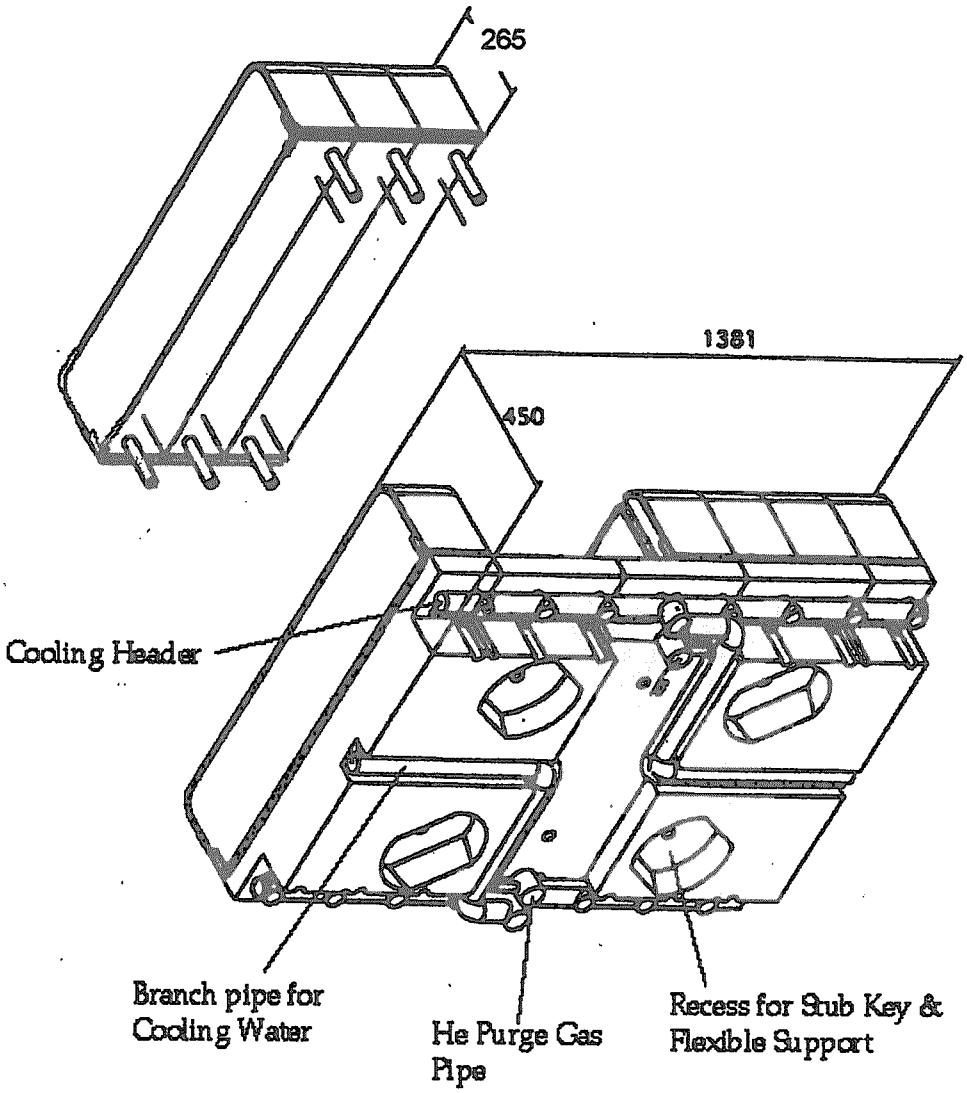

Fig. 4-2 Rear Side View of the ITER Breeding Blanket

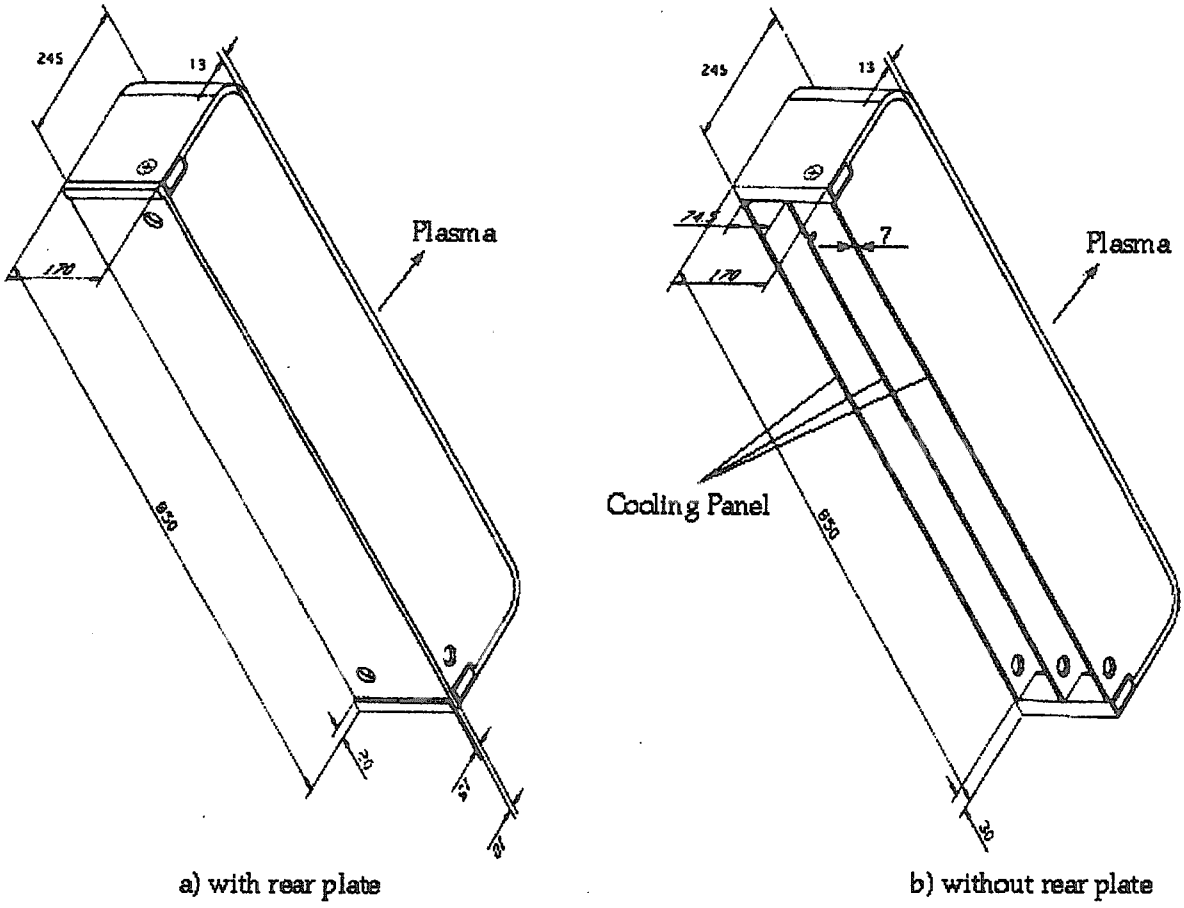

a) with rear plate b) without rear plate

Fig. 4-3 Structure of the Breeding Cell of the ITER Breeding Blanket

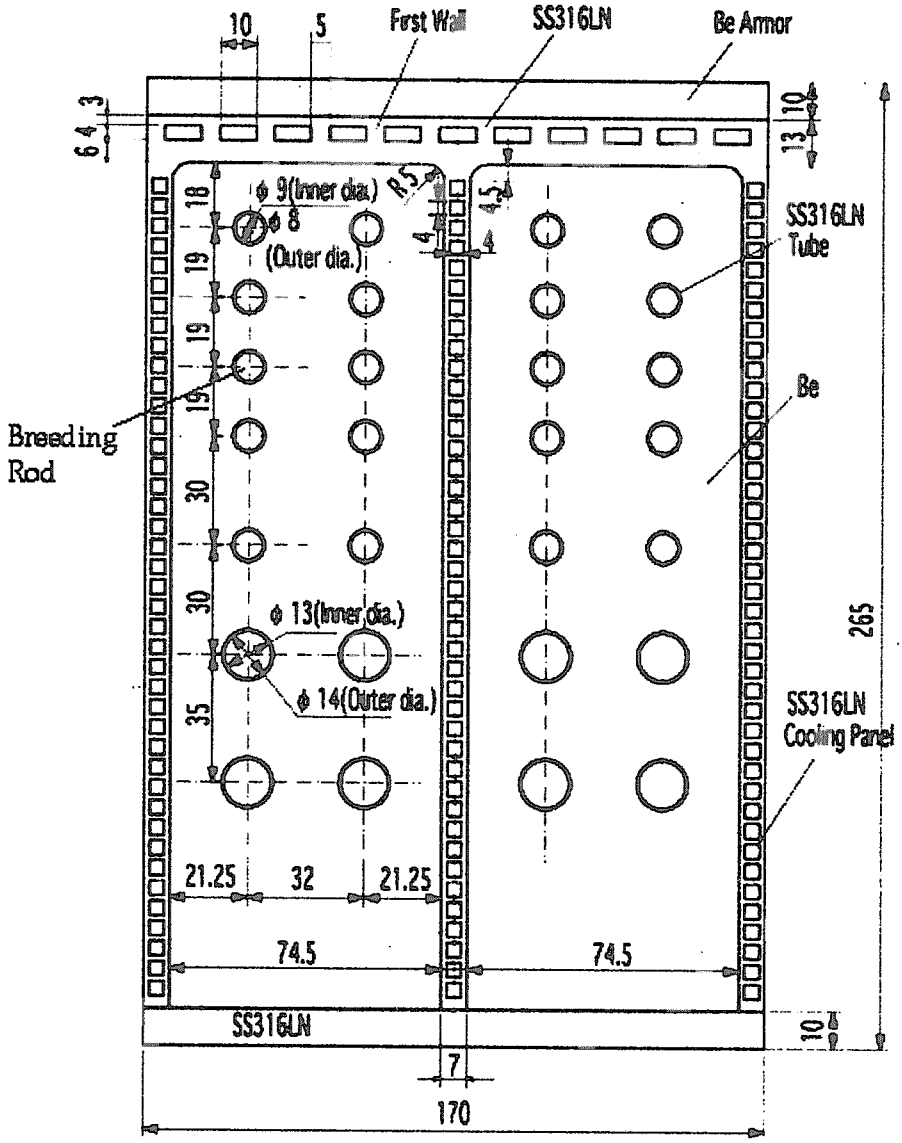

Fig. 4-4 Cross Section of the Breeding Cell of the ITER Breeding Blanket

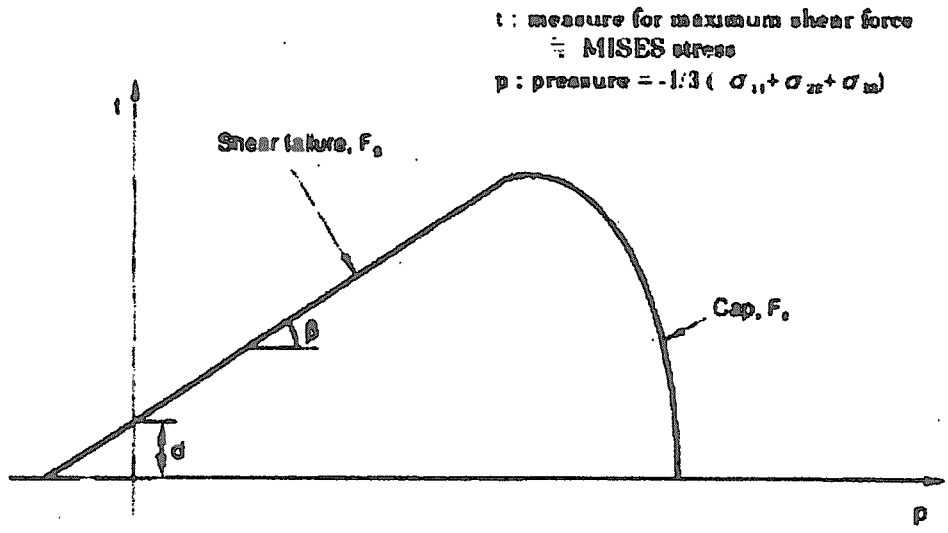

a) yield surface

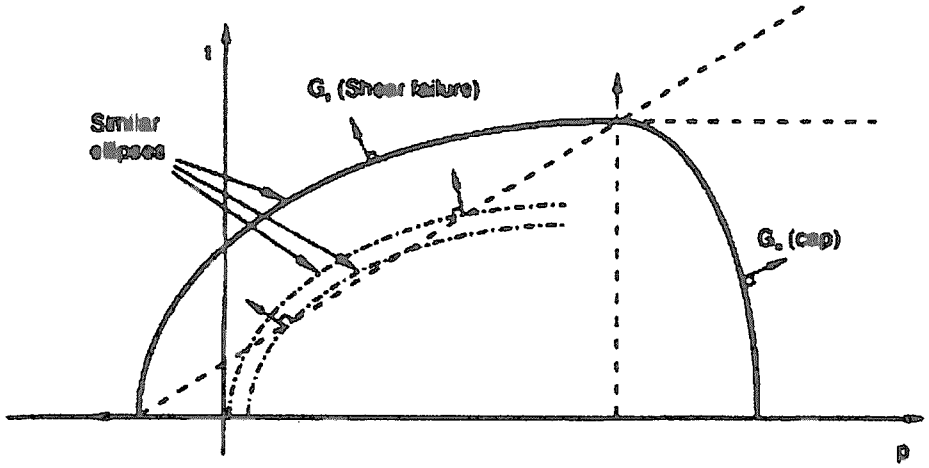

b) flow potential

Fig. 4-5 Modified Drucker-Prager/Cap model of the yield surface and flow potential of the packed bed

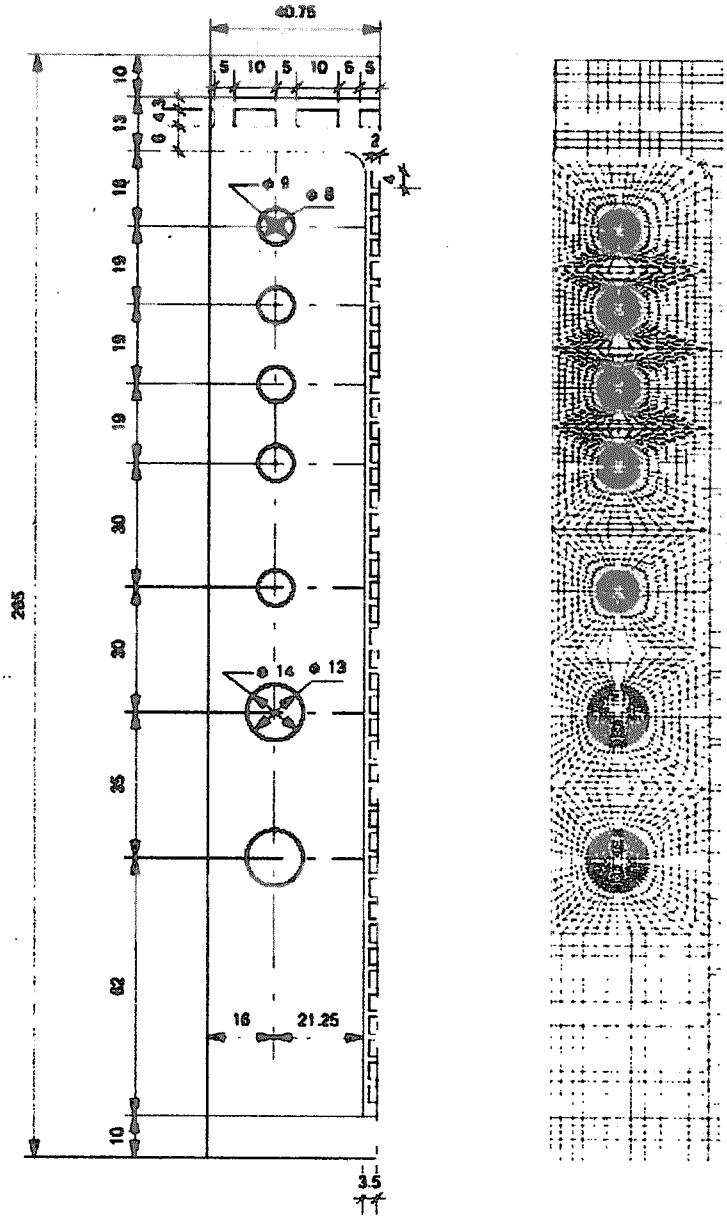

Fig. 4-6 Analysis model of a breeding cell for a finite element method analysis

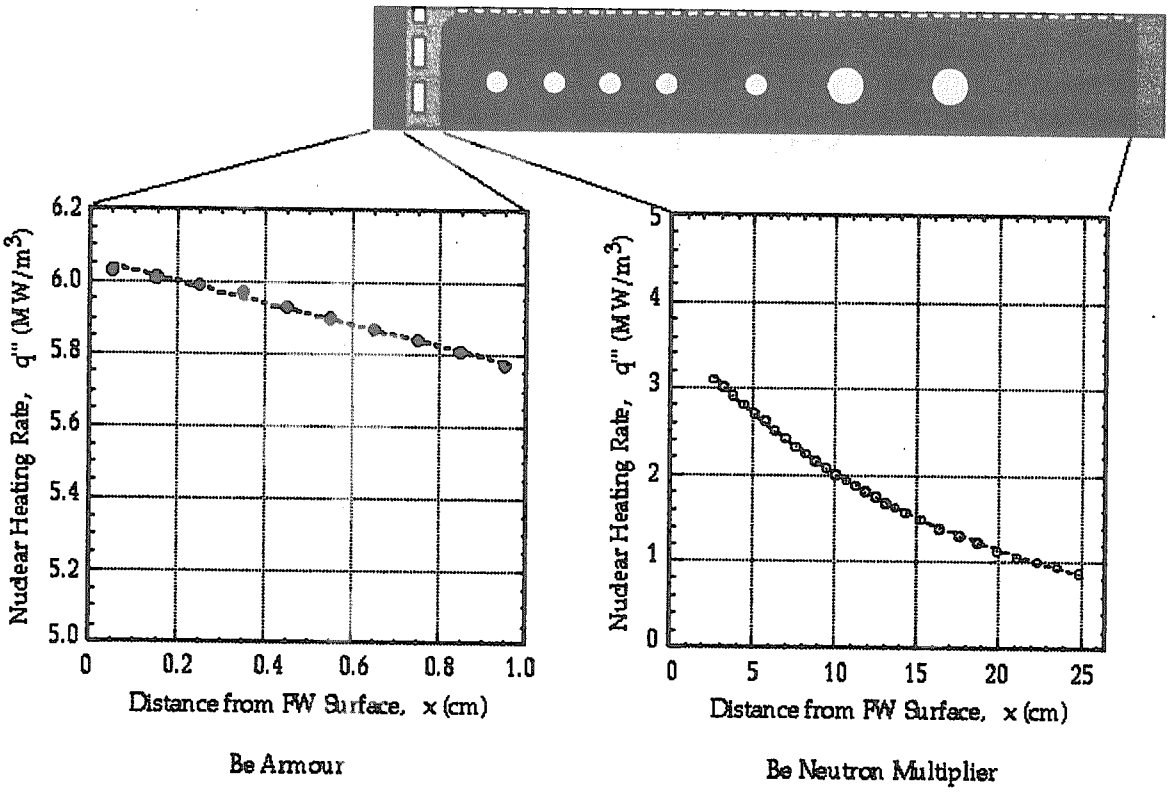

Fig. 4-7 Nuclear heating rate of beryllium armor and neutron multiplier pebble bed

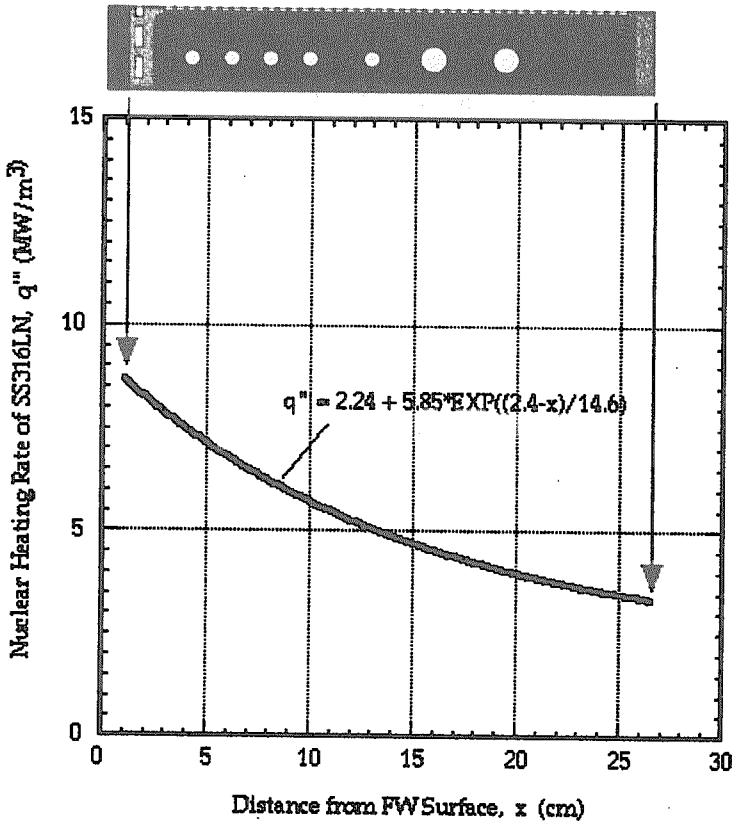

Fig. 4-8 Nuclear heating rate of stainless steel

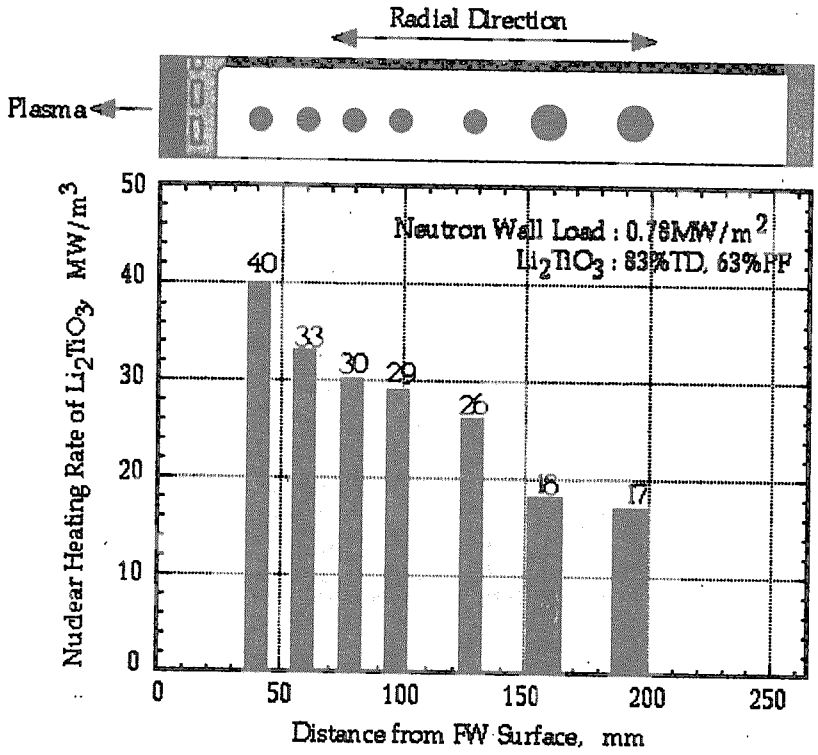

Fig. 4-9 Nuclear heating rate distribution of breeder pebble bed by the location of breeder rod

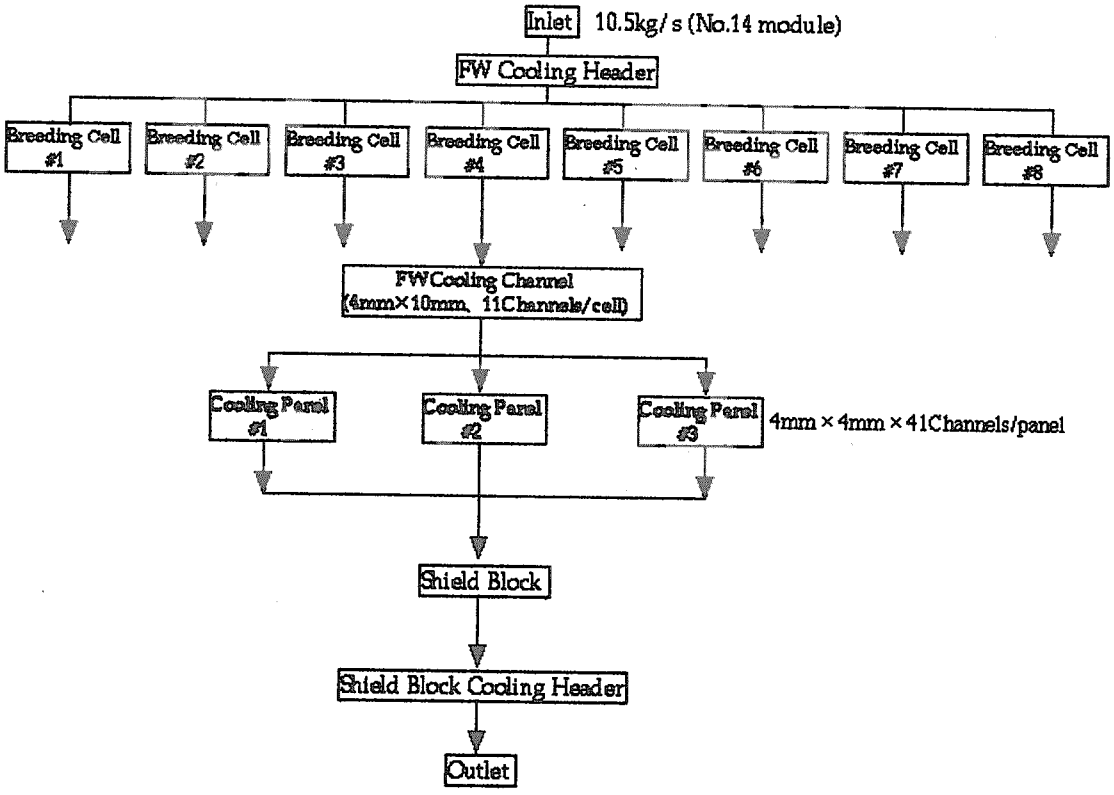

Fig. 4-10 Schematic coolant flow diagram for the ITER breeding blanket

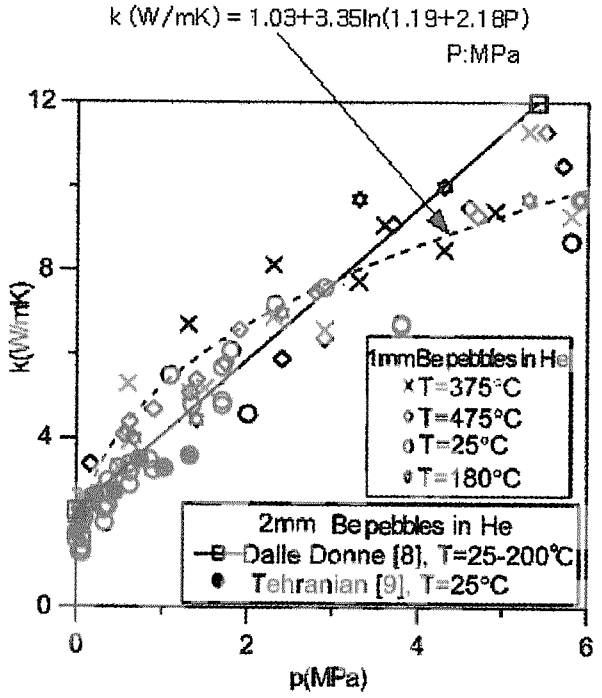

Fig. 4-11 Pebble bed thermal conductivity as a function of compressive stress in the pebble bed [19]

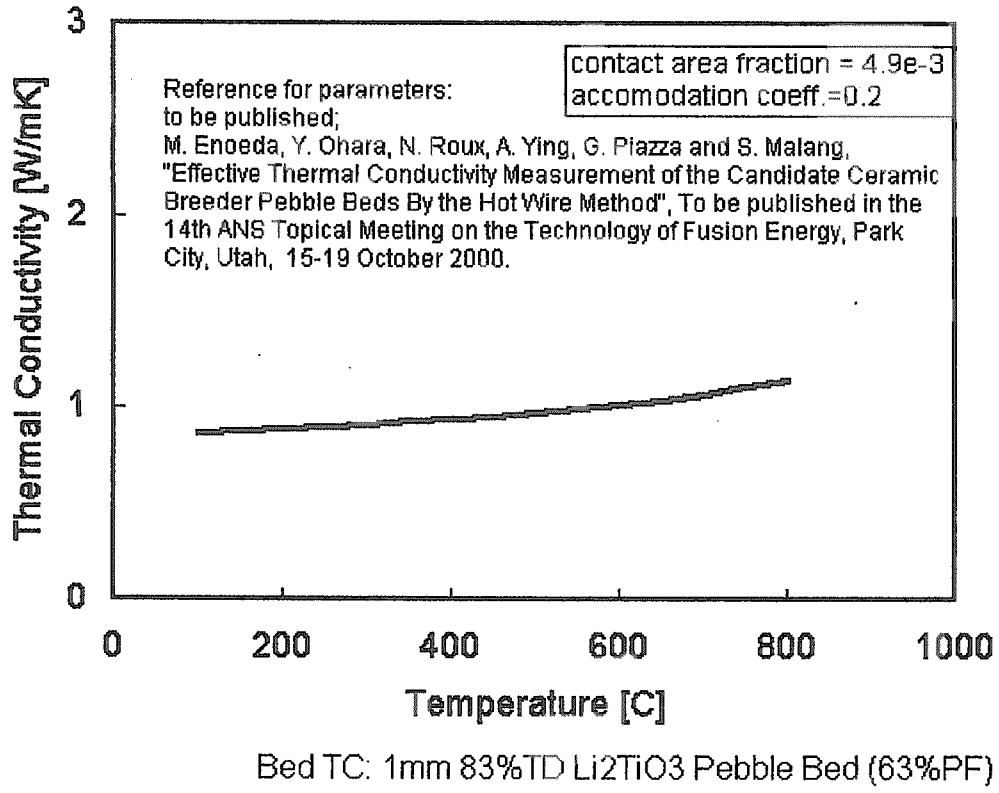

Fig. 4-12 Pebble bed thermal conductivity of Li_2TiO_3 [21]

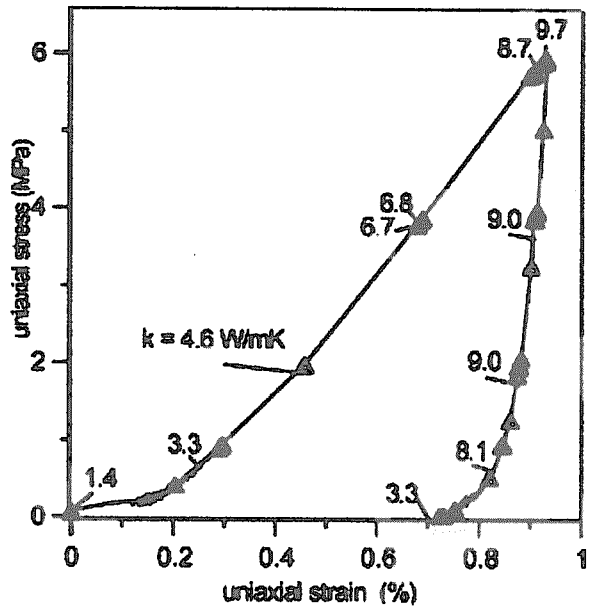

Fig. 4-13 Stress-Strain curve and effective thermal conductivity of Be pebble bed [19]

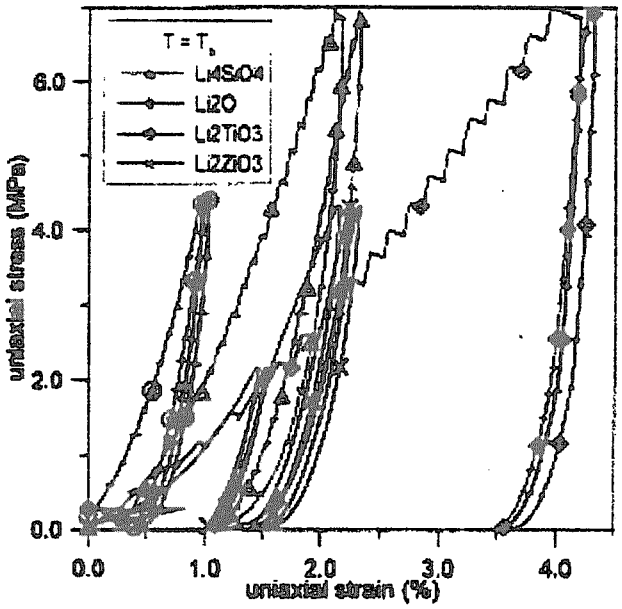

Fig. 4-14 Stress-Strain curve of Li_2TiO_3 pebble bed [22]

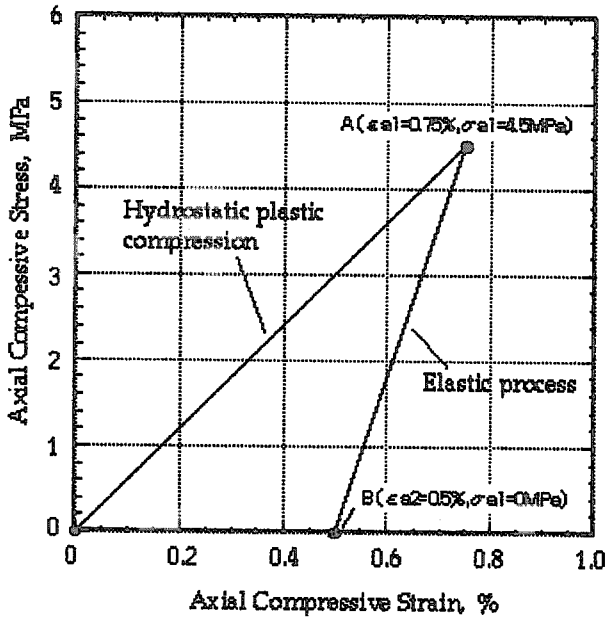

Fig. 4-15 Relationship between axial stress and axial strain of Li_2TiO_3 pebble bed

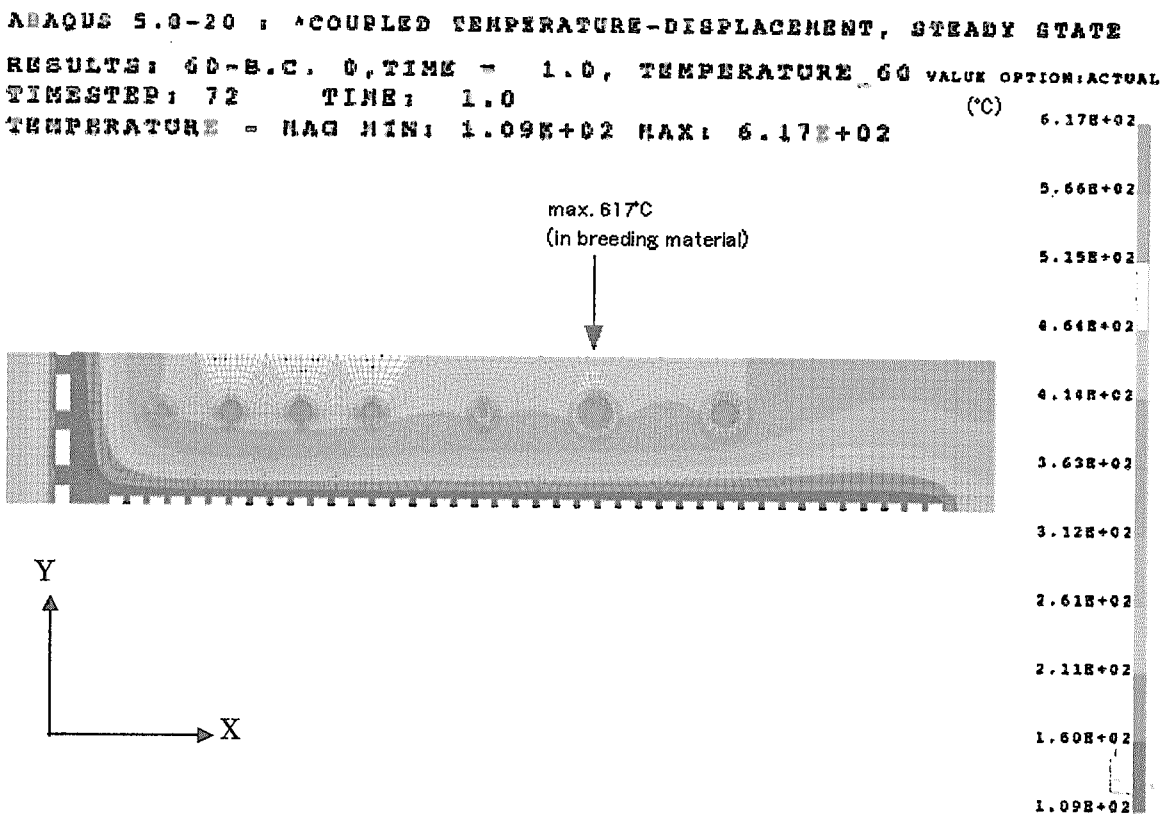

Fig. 4-16 Temperature distribution in the breeding cell

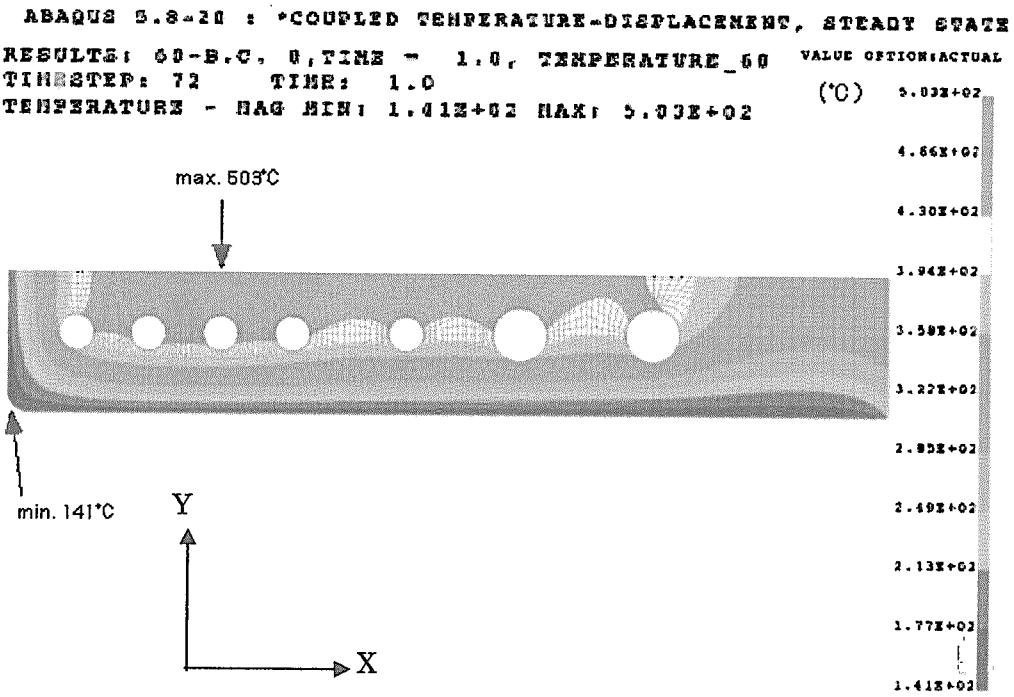

Fig. 4-17 Temperature distribution in the multiplier pebble bed in the breeding cell

This is a blank page.

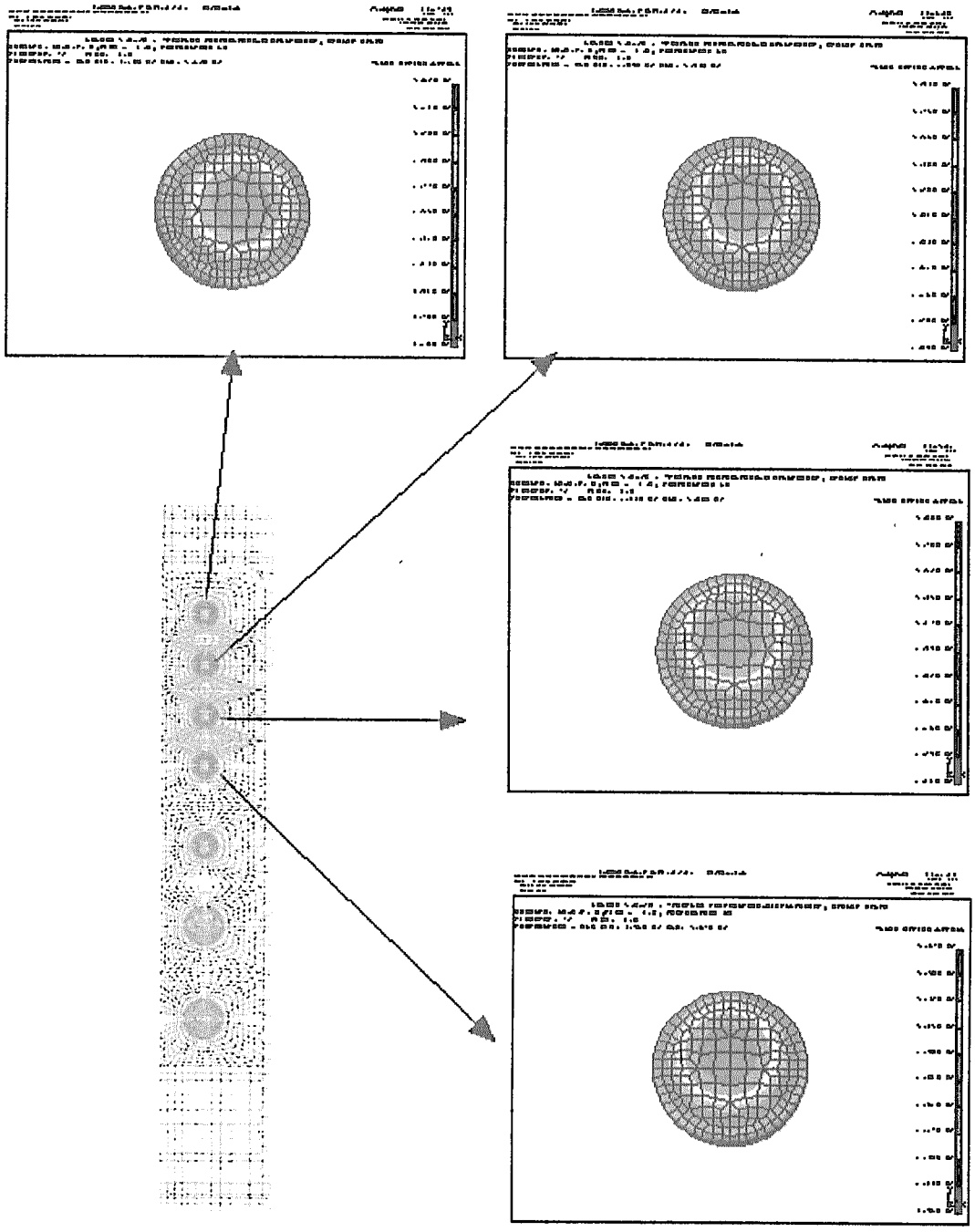

Fig. 4-18 Temperature distribution in the breeder pebble beds in 1st row to 4th row of the breeder rods

This is a blank page.

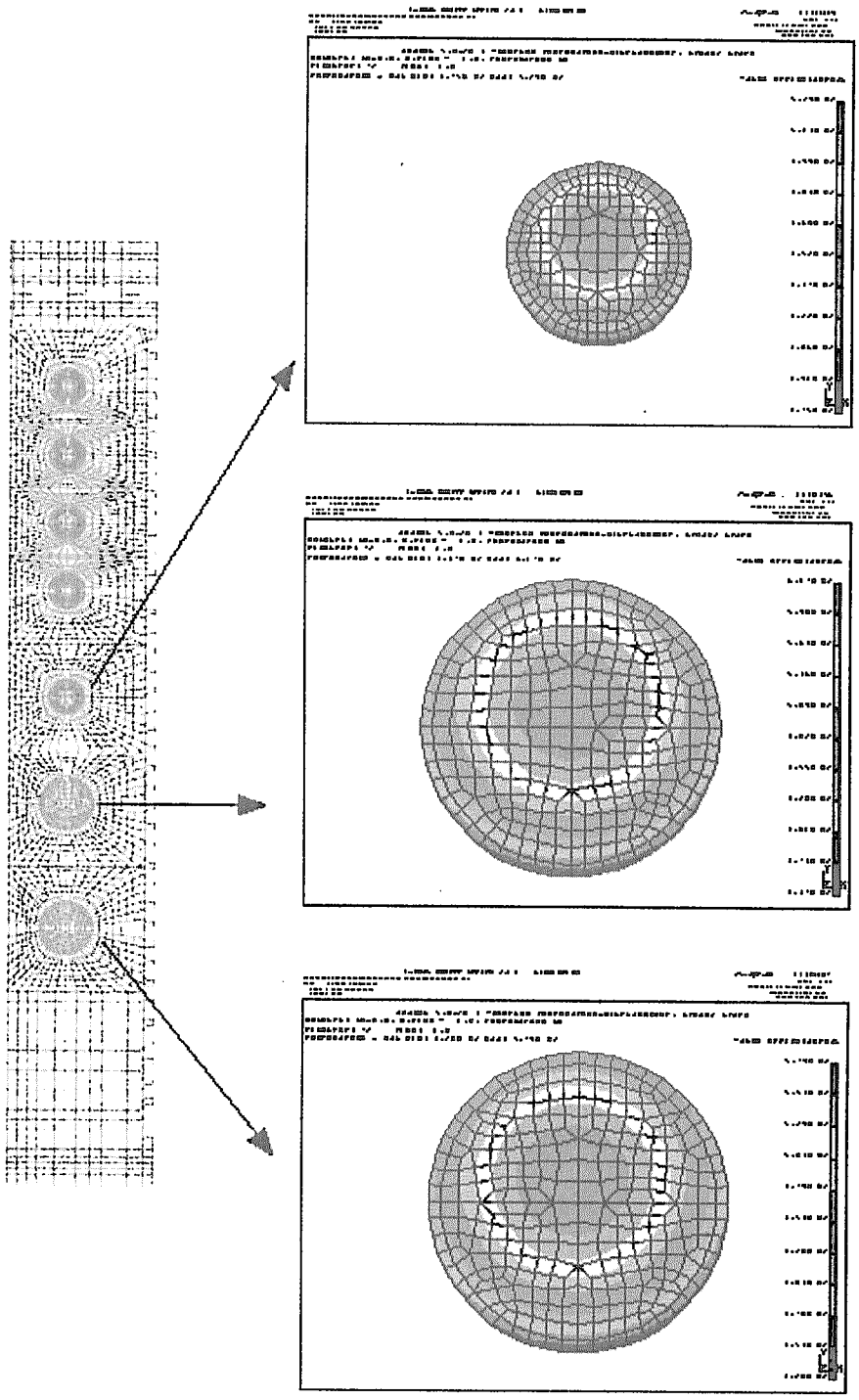

Fig. 4-19 Temperature distribution in the breeder pebble bed in 5th row to 7th row of the breeder rods

This is a blank page.

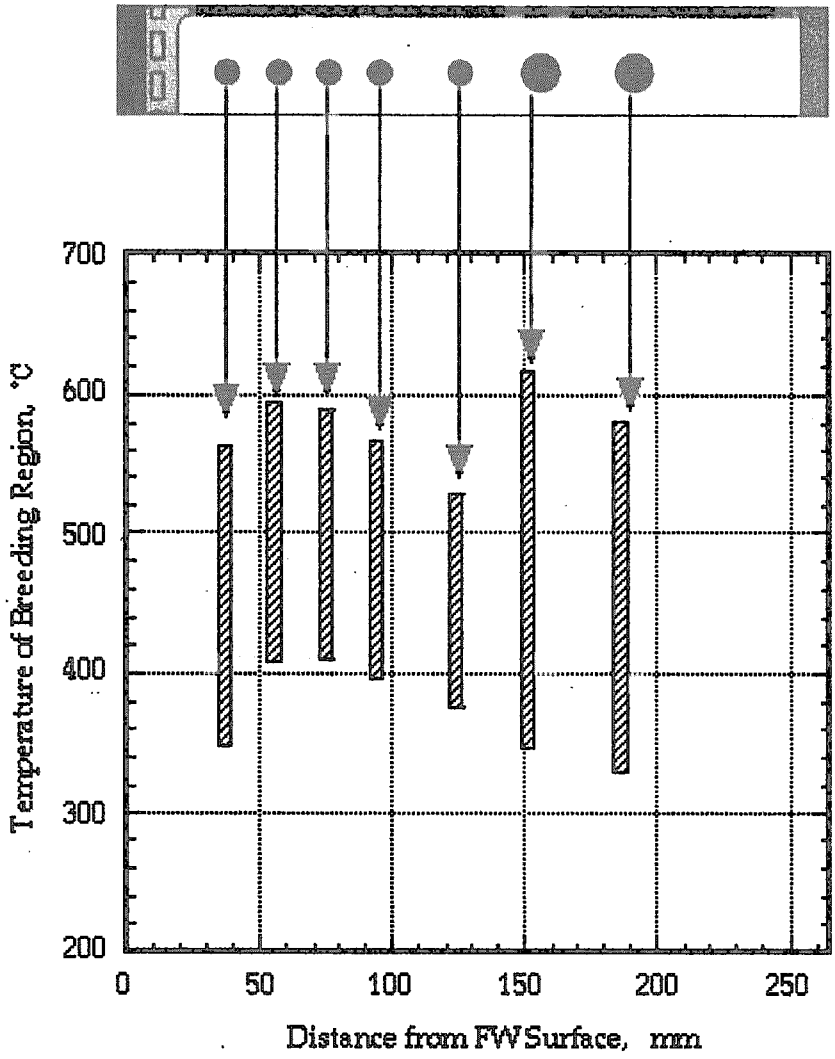

Fig. 4-20 Temperature ranges of the breeder pebble beds in the breeder rods

This is a blank page.

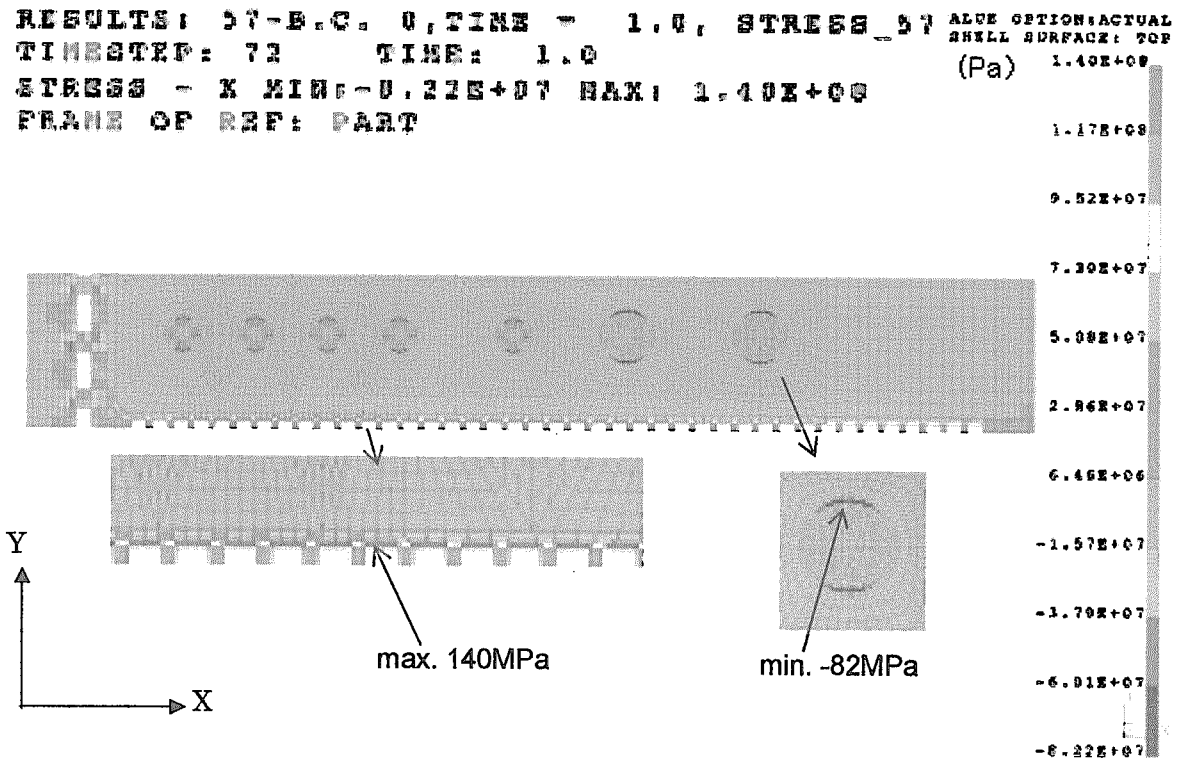

Fig. 4-21 Distribution of x component stress in the breeding cell

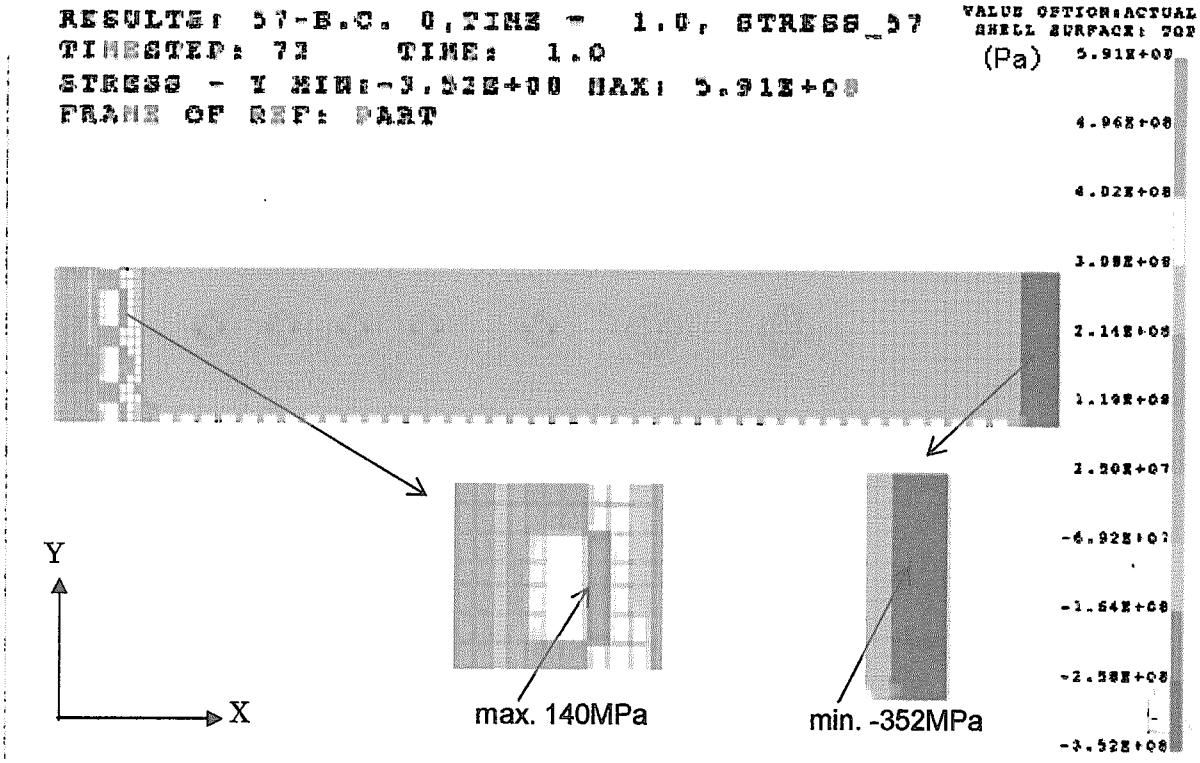

Fig. 4-22 Distribution of y component stress in the breeding cell

This is a blank page.

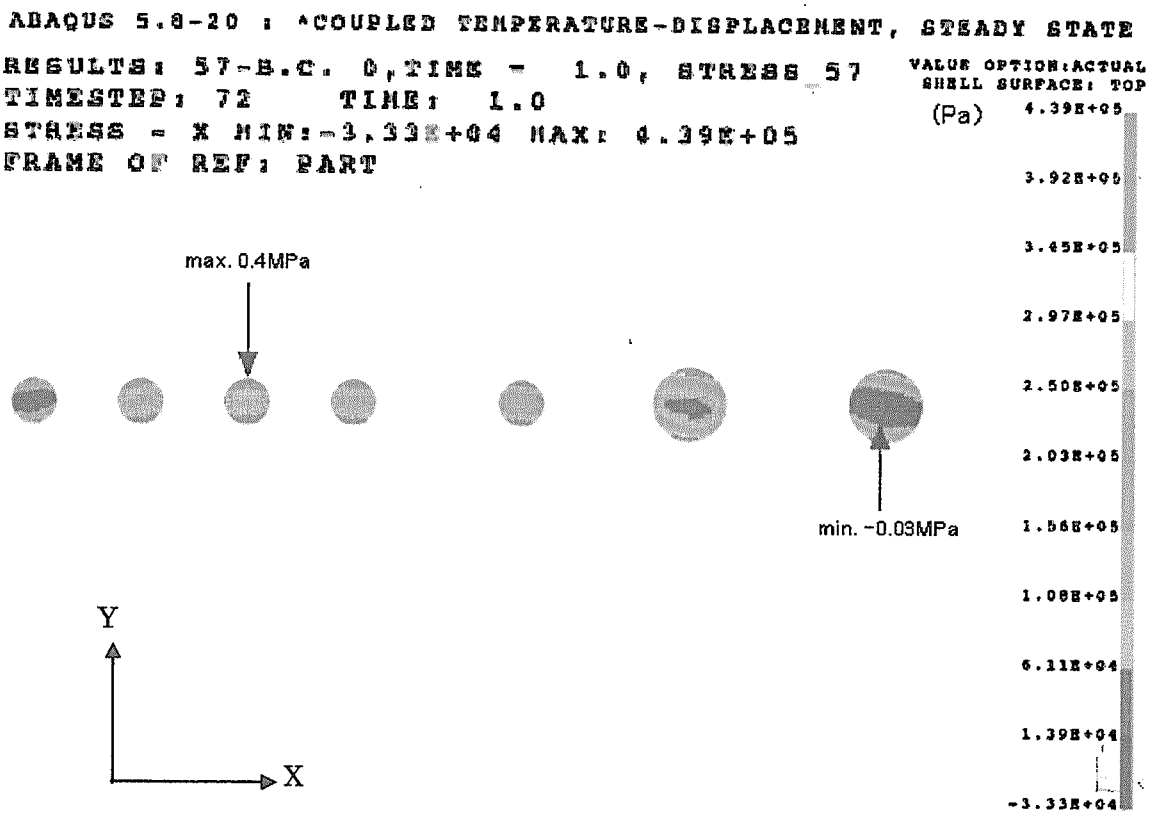

Fig. 4-23 Distribution of x component stress in the breeder pebble beds in the breeder rods

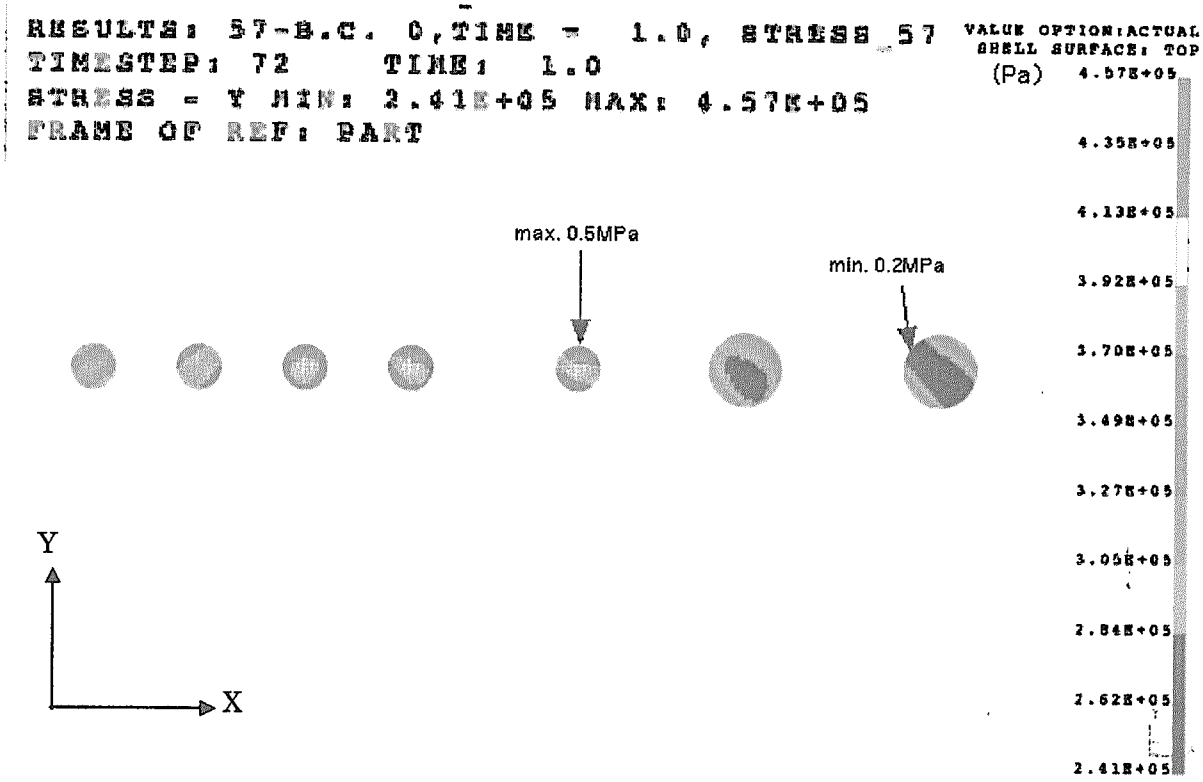

Fig. 4-24 Distribution of y component stress in the breeder pebble beds in the breeder rods

This is a blank page.

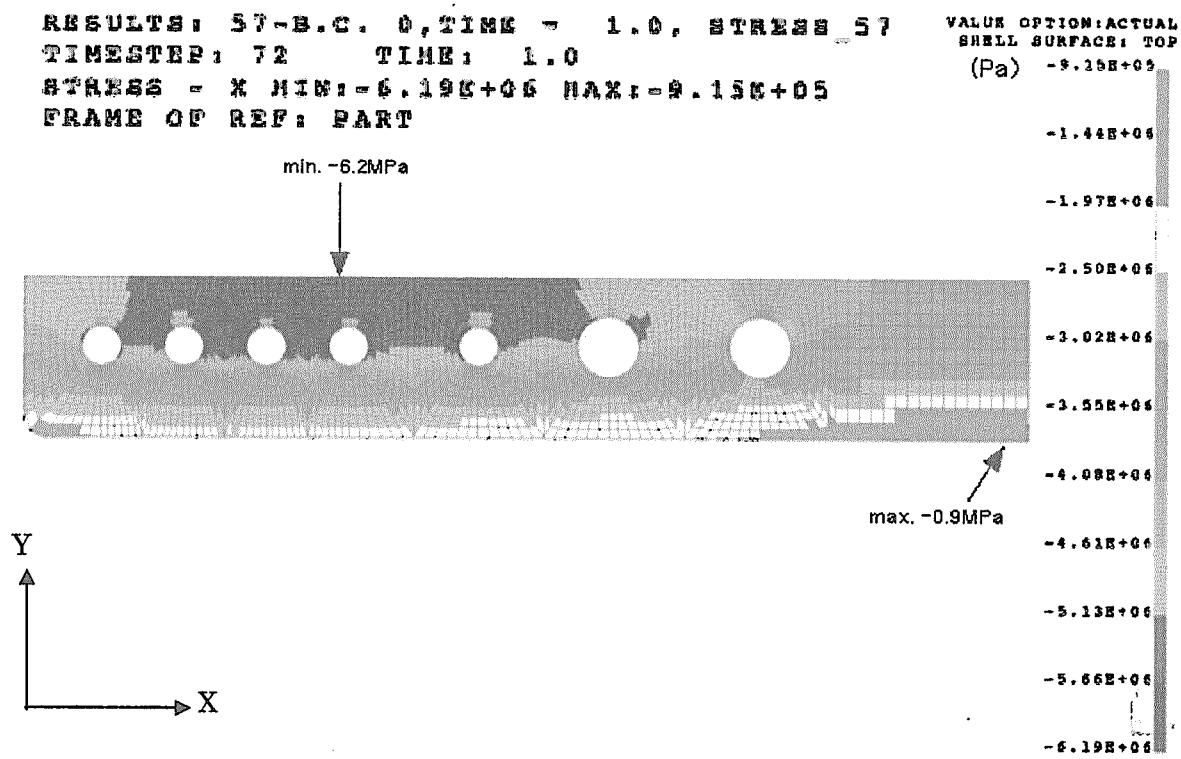

Fig. 4-25 Distribution of x component stress in the multiplier pebble bed in the breeder cell

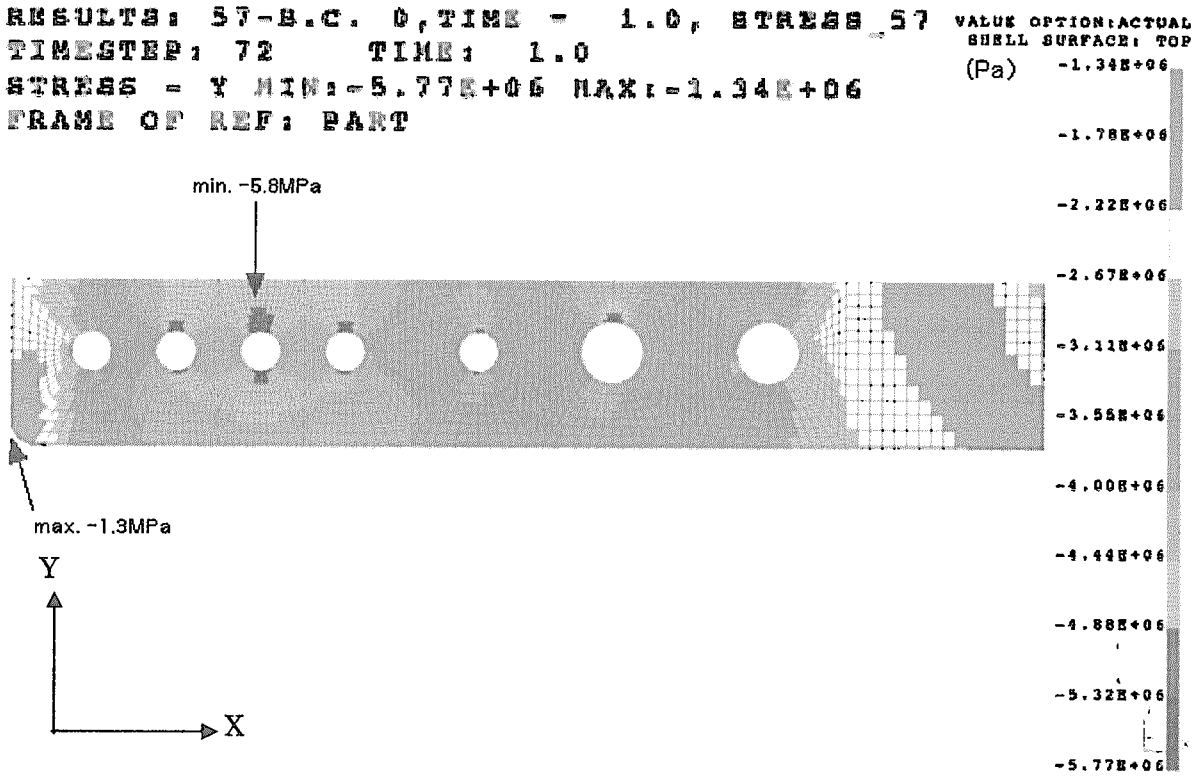

Fig. 4-26 Distribution of y component stress in the multiplier pebble bed in the breeder cell

This is a blank page.

5. Conclusions

The analyses performed in this study showed the justification and possible improvement on the design of the ITER breeding blanket, from the view points of tritium breeding performance, tritium release performance and thermo-mechanical performance. Major results are concluded as follows.

(1) The detailed analyses of the distribution of the nuclear heating rate and TBR have been performed in 2D model using MCNP to identify the detailed tritium inventory and release rate analyses and thermo-mechanical analyses.
(2) The parametric analyses for selection of purge gas flow rate were carried out from the view point of pressure drop and the tritium inventory and release control of Li_2TiO_3 breeder. The analysis result concluded that purge gas flow rate can be set to conventional flow rate setting (88 l/min per module) to 1/10 of that to save the purge gas flow and minimize the size of purge gas pipe.
(3) Thermo-mechanical analyses of the pebble bed blanket structure, by ABAQUS with 2D model, have been performed to identify the temperature distribution incorporating the pebble bed mechanical simulation and influence of mechanical behavior to the thermal behavior. The result clarified that temperature and stress are acceptable from the view points of material and functional soundness.

Additionally, the effect of Be multiplier elimination on total TBR was studied as a basic parameter study by one dimensional analysis using ANISN. It was estimated that total TBR decreases 30 % from the total TBR of the ITER breeding blanket with Be pebble.

Acknowledgement

The authors wish to express sincere appreciation to Dr. Masahiro Seki, Dr. Hideyuki Takatsu and Dr. Shogo Seki for their continuous encouragement. Also, the authors wish to express special gratitude to Dr. Kimihiro Ioki and Dr. Masao Yamada of ITER JCT for their guidance of design work.

References

[1] ITER Design Description Document G 16DDD XX 01-06-07 W 0.1, Section 1.2 Page 115-147.

[2] P. C. Carman, Trans. Inst. Chem. Engrs. (London), 23, 150 (1937)

[3] M. Nishikawa, A. Baba, S. Odoi, Y. Kawamura, "Tritium Inventory estimation in Solid Blanket System", F. E. D., 39-40 (1998) 615 - 625.

[4] A. Baba, M. Nishikawa, Y. Kawamura, K. Okuno, "Isotope Exchange Reaction of Solid Breeder Materials", Journ. Nucl. Mater., 248 (1997) 106-110.

[5] K. Munakata, M. Nishikawa, K. Yoneda, "Effect of Water in an Li_2O Bed on Tritium Inventory", Fusion Technol., Vol. 15 (1989) 1451.

[6] Y. Kawamura, M. Nishikawa, K. Tanaka, "Adsorption Characteristics of Water Vapor on Li_4SiO_4", Journ. Nucl. Mater., 208 (1994) 308-312.

[7] Y. Kawamura, M. Nishikawa, K. Tanaka, "Adsorption Characteristics of Water Vapor on Li_2ZrO_3", Journ. Nucl. Mater., 218 (1994) 57-65.

[8] K. Munakata and M. Nishikawa, "Isotope Exchange Reaction on Lithium Oxide", Journ. Nucl. Mater., 170 (1990) 187-192.

[9] Y. Kawamura, M. Enoeda, K. Okuno, "Isotope Exchange Reaction in Li_2ZrO_3 packed bed", F. E. D., 39-40 (1998) 713-721.

[10] A. Baba, M. Nishikawa, T. Eguchi, "Isotope Exchange Reaction on Li_2ZrO_3", Journ, Nucl. Mater., 250 (1997) 29-35.

[11] M. Nishikawa, A. Baba, Y. Kawamura, M. Nishi, "Isotope Exchange Reactions on Ceramic Breeder Materials and their effect on Tritium Inventory", JAERI-Conf 98-006 (1998) 170.

[12] H. Kudo, K. Okuno, S. O'hira, "Tritium Release Behavior of Ceramic Breeder Candidates for Fusion Rectors", Journ. Nucl. Mater., 155-157 (1988) 524-528.

[13] M. Nishikawa, S. Beloglazov, T. Kawagoe, N. Nakajima, A. Baba, "Isotope Exchange Reaction 1 in Li_2TiO_3 Placed in H2 Atmosphere at High Temperature", Proceedings of the Ninth International Workshop on Ceramic Breeder Blanket Interactions, Sept. 27-29 2000, Toki, Japan, (2000) 163.

[14] T. Tanifuji, D. Yamaki, S. Nasu, K. Noda, "Tritium Release Behavior from Neutron-Irradiated Li_2TiO_3 Single Crystal", JAERI-Conf 98-006 (1998) 200.

[15] H. C. Urey, " The Thermodynamic Properties of Isotopic Substances", J. Chem. Soc., (1947) 562.

[16] ITER Plant Description Document (PDD), G A0 FDR 1 00-11-16 W0.1

[17] Hibbit, Karlsson & Sorensen, Inc., ABAQUS User's Manual - version 5.8

[18] S.Kikuchi et al., Preliminary Thermo-Mechanical Analysis of ITER Breeding Blanket, JAERI-Tech 98-059, 1999

[19] J.Reimann et al., Thermal Conductivity measurements of deformed beryllium Pebble Beds By Hot Wire Method, CBBI-9, Sept.27-29, 2000

[20] E.U. Schlunder and R.Bauer, Inter. Chem. Eng. 18 (1978), 181

[21] M.Enoeda, Y.Ohara, N.Roux, A.Ying, G.Piazza and S.Malang, "Effective Thermal Conductivity Measurement of the Candidate Ceramic Breeder Pebble Beds By the Hot

Wire Method", To be published in the 14th ANS Topical Meeting on the Technology of Fusion Energy, Park City, Utah, 15-19 October 2000.

[22] J.Reimann et al., Thermomecanical behaviour of ceramic breeder and beryllium pebble beds, Fusion Engineering and Design 49-50, 643-649, 2000

[23] ITER Design description Document, 1.6B Breeder Blanket System, G16 DDD 2 98-06-10 W0.4

Appendix 1

A1. TBR and Temperature Analyses for No Neutron Multiplier Configuration

A1.1 Objectives

A neutron multiplier Be is applied as a pebble bed in the ITER breeding blanket design. Be multiplier has reactivity with high temperature water and produces hydrogen. From the safety point of view, the breeding blanket without Be multiplier would have advantage if tritium breeding performance is not significantly degraded. In this analysis, tritium breeding ratio (TBR) of the breeding blanket without Be multiplier is estimated by 1D nuclear analysis for the feasibility study of the blanket design without neutron multiplier Be.

A1.2 Analysis

(a) Geometry

The reference design is shown in Fig. A1-1. A method of modeling the blanket design into 1D geometry is shown in Fig. A1-2a. A concept of the design without Be pebble bed is also shown in this figure. Each layer has a composition with mixed materials. The composition and thickness of each layer is shown in Table A1-1. The width of Li_2TiO_3 pebble bed of the design without Be is calculated to be 16 mm as shown in Fig. A1-2b. A temperature distribution of infinite plain with uniform-volumetric-heating source and cooling panel is given by

$$\Delta T = q''' a^2 / 2\lambda$$

Where

q''' : volumetric heating rate

a : width of Li_2TiO_3 pebble bed

λ: equivalent thermal conductivity of Li_2TiO_3 pebble bed

λ is estimated to be 1.1 W/mK by SZB correlation.

IF ΔT is assumed to be 300 °C and q''' is to be 10 MW/m^3, width of pebble bed 2a results in 16 mm.

(b) Analysis method

Nuclear analyses were carried out by using 1-D S_N code ANISN with the group constant set FUSION-40 based on JENDL-3. Conditions for 1D nuclear analysis are shown in Table 3-2. The Li_2TiO_3 is selected as a breeding material and assumed to be binary pebble bed packed at fraction of 75% for both cases. Be pebble bed is assumed to be contained as binary pebble bed at fraction of 80%.

Table A1-1 Composition and thickness of 1D model

No.	1	2	3	4	5	6	7	8	9	10
distance from surface(mm)	0	5	8	12	18	28	37	47	56	66
thickness(mm)	5	3	4	6	10	9	10	9	10	9
composition(%)	Be(100)	SS(100)	SS(42) Water(58)	SS(100)	Be(90) SS(10)	Breeder(16) Be(70) SS(10) Water(4)	Be(90) SS(6) Water(4)	Breeder(16) Be(70) SS(10) Water(4)	Be(90) SS(6) Water(4)	Breeder(16) Be(70) SS(10) Water(4)

No.	11	12	13	14	15	16	17	18	19	20
distance from surface(mm)	75	86	95	113	122	142.5	156.5	177	191	205.5
thickness(mm)	11	9	18	9	20.5	14	20.5	14	14.5	14
composition(%)	Be(90) SS(6) Water(4)	Breeder(16) Be(70) SS(10) Water(4)	Be(90) SS(6) Water(4)	Breeder(16) Be(70) SS(10) Water(4)	Be(90) SS(6) Water(4)	Breeder(28) Be(58) SS(10) Water(4)	Be(90) SS(6) Water(4)	Breeder(28) Be(58) SS(10) Water(4)	Be(90) SS(6) Water(4)	Breeder(28) Be(58) SS(10) Water(4)

No.	21	22
distance from surface(mm)	219.5	264.5
thickness(mm)	45	30
composition(%)	Be(90) SS(6) Water(4)	SS(100)

Table A1-2 Conditions for 1D nuclear analyses

	With Be	Without Be	Comments
Coolant Temperature	150°C		
Breeder Theoretical density Porosity Packing fraction Thermal conductivity of material Thermal conductivity of pebble bed ^{6}Li enrichment Maximum temperature	Li_2TiO_3 3.44g/cm^3 15% binary 2mm : 60%, 0.2mm : 15% 2.1～2.4W/(m･K) 1.1 - 1.2*W/m K Natural,30% <1000°C		
Neutron multiplier Density Packing fraction Thermal conductivity of material	Be 1.84g/cm^3 binary 2mm : 60% 0.2mm : 20% 12.6 - 12.7**W/m K	-	
Neutron wall loading	0.78(MW/m^2)		

* estimated by SZB correlation

** estimated based on FZK experiments at ε=0.1%

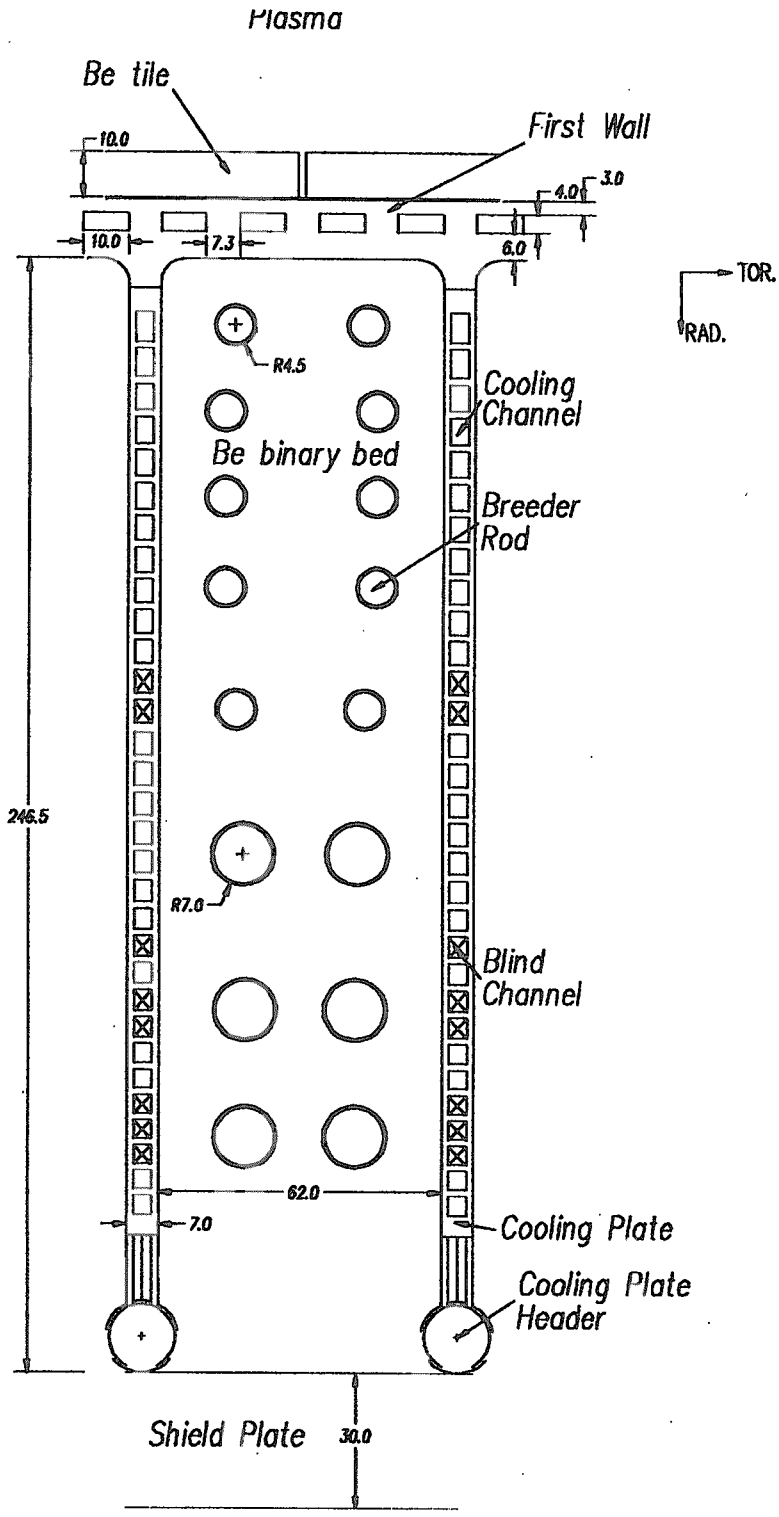

Fig. A1-1 ITER breeding blanket design

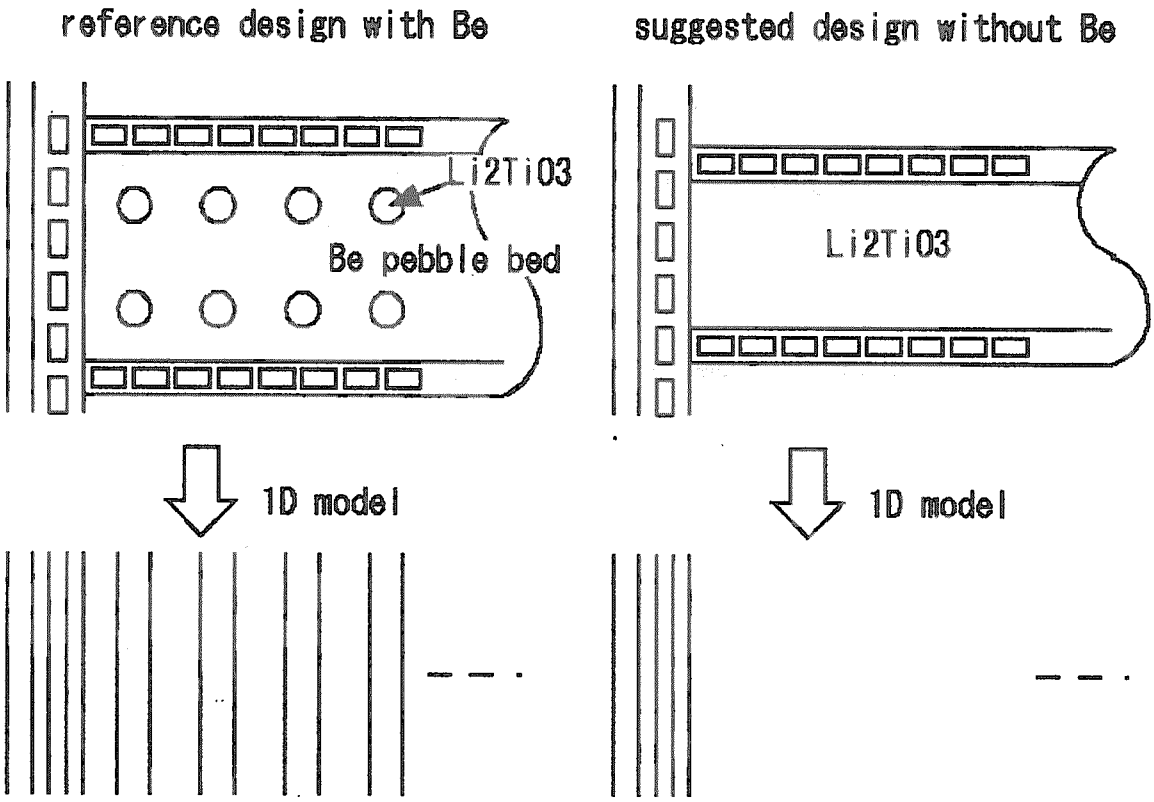

Fig. A1-2a Calculation model and homogenization for 1D TBR calculation

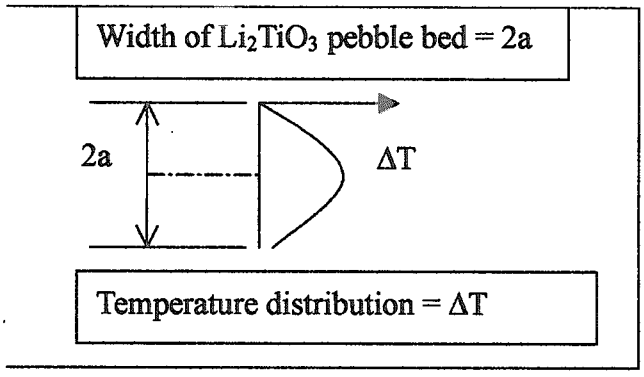

Fig. A1-2b Determination of Li_2TiO_3 width without Be design

A1.3 Results

Neutron flux distributions of the reference blanket and the blanket without Be multiplier are shown in Fig. A1-3a and A1-3b, respectively. The reference blanket has the higher thermal neutron flux than the later blanket because of the neutron multiplier. The volumetric heating rate of reference blanket and suggested blanket without Be are shown in Fig. A1-4a and A1-4b, respectively. The maximum volumetric heating rate is reached to be 10 MW/m^3 in the breeder rod region of the reference blanket. In the case of the suggested blanket it is as much as 8 MW/m^3. This means that the $10MW/m^3$ applied for calculating the width of Li_2TiO_3 pebble bed is suitable. The local TBR of reference blanket and of suggested blanket without Be are shown in Fig. A1-5a and A1-5b, respectively. The dependence of TBR on 6Li enrichment is summarized in Table A1-3. The local TBR of the blanket without Be is produced as much as 0.88 in 30 % ^6Li enrichment case and can reach more than 70 % of that of the reference blanket.

A1.4 Conclusion

The breeding blanket design without neutron multiplier Be is proposed and the TBR is estimated to be about 70% of the reference blanket. The possibility could be remained for one of candidates as alternatives of ITER breeding blanket if the system safety is considered to be primary issue.

Table A1-3 Local TBR of reference blanket and of suggested blanket

		Natural enrichment	30% ^6Li enrichment
Reference blanket	^6Li	0.94	1.19
	^7Li	0.01	0.01
	total	0.95	1.19
Suggested blanket without Be	^6Li	0.74	0.84
	^7Li	0.06	0.04
	total	0.80	0.88

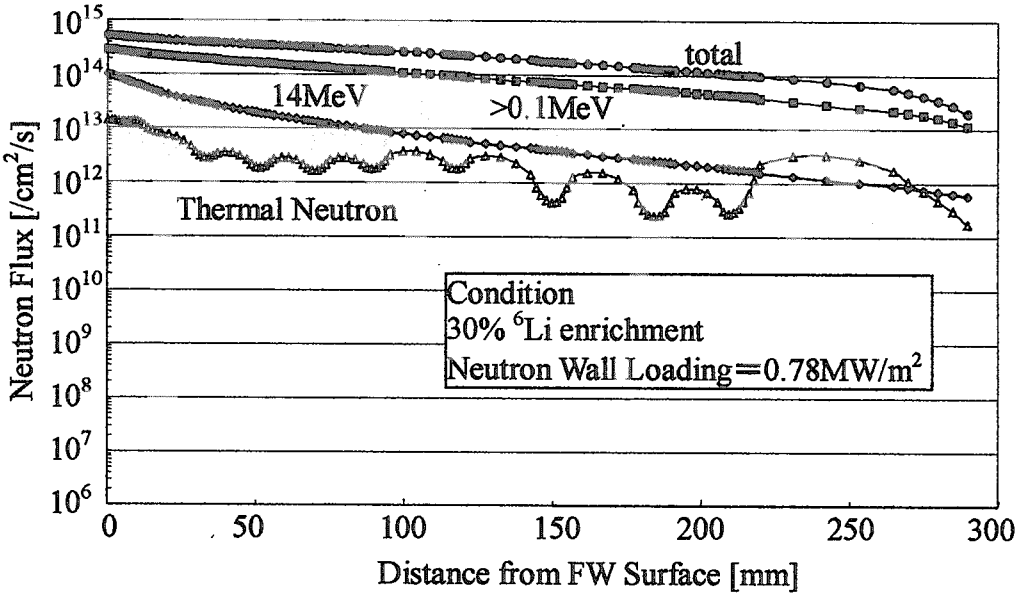

Fig. A1-3a Neutron Flux Distribution of Reference Blanket

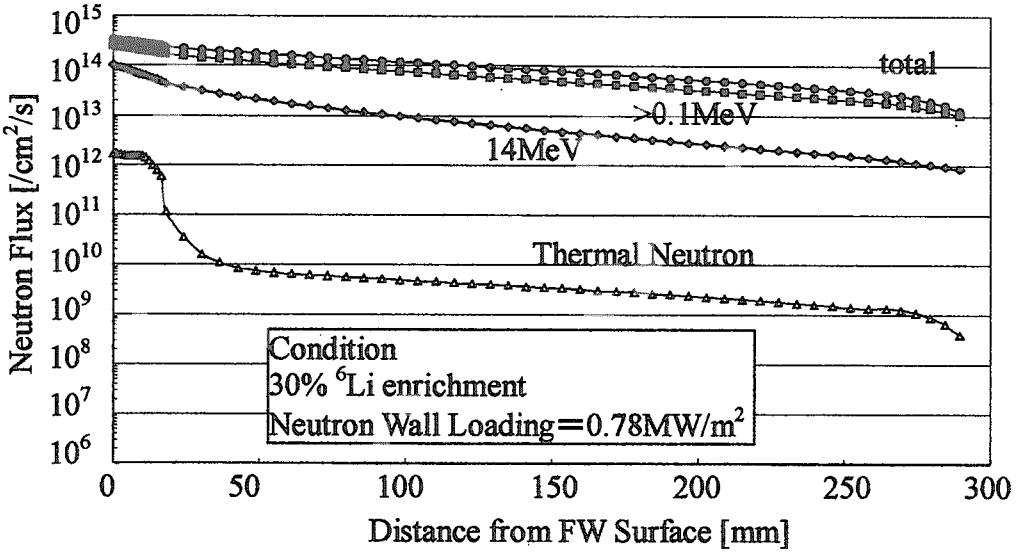

Fig. A1-3b Neutron Flux Distribution of Suggested Blanket without Be

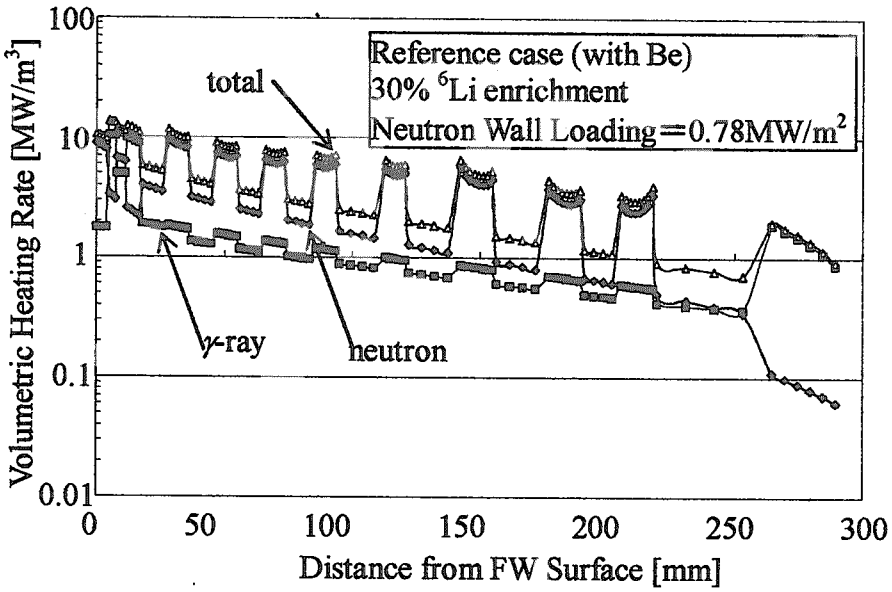

Fig. A1-4a Volumetric Heating Rate Distribution of Reference Blanket

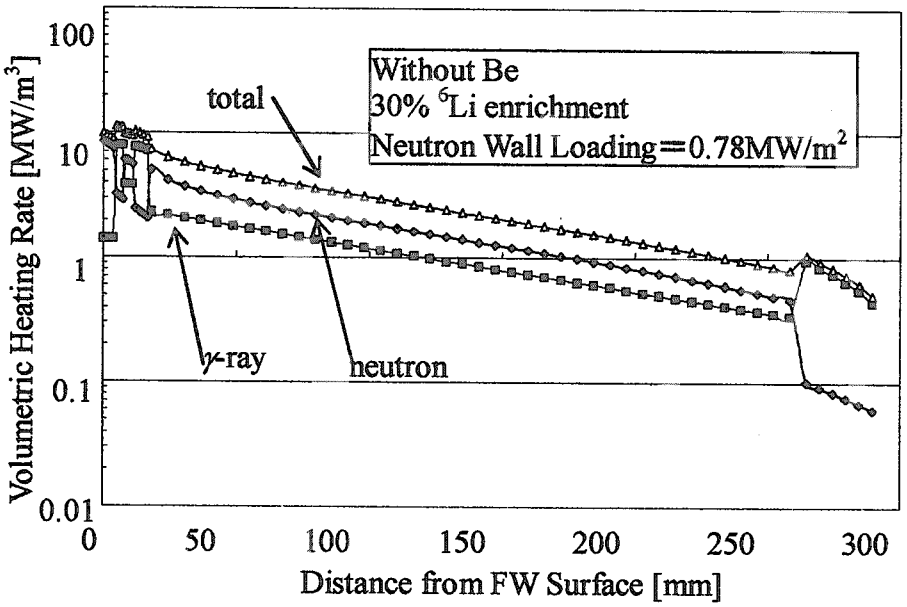

Fig. A1-4b Volumetric Heating Rate Distribution of Suggested Blanket without Be

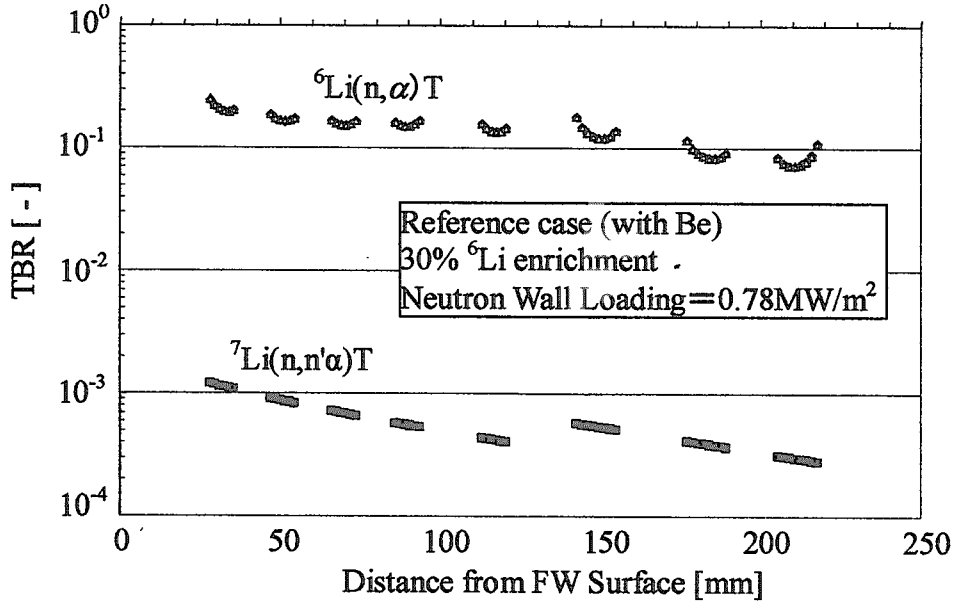

Fig. A1-5a TBR Distribution of Reference Blanket

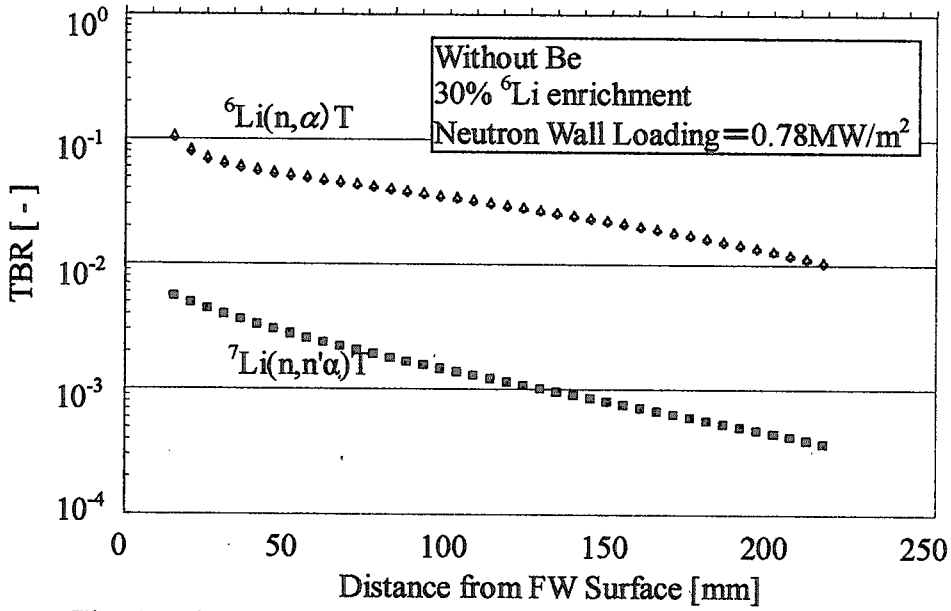

Fig. A1-5b TBR Distribution of Suggested Blanket without Be

This is a blank page.

国際単位系（SI）と換算表

表1　SI基本単位および補助単位

量	名称	記号
長さ	メートル	m
質量	キログラム	kg
時間	秒	s
電流	アンペア	A
熱力学温度	ケルビン	K
物質量	モル	mol
光度	カンデラ	cd
平面角	ラジアン	rad
立体角	ステラジアン	sr

表2　SIと併用される単位

名称	記号
分，時，日	min, h, d
度，分，秒	°, ′, ″
リットル	l, L
トン	t
電子ボルト	eV
原子質量単位	u

1 eV=1.60218×10^{-19}J

1 u=1.66054×10^{-27}kg

表3　固有の名称をもつSI組立単位

量	名称	記号	他のSI単位による表現
周波数	ヘルツ	Hz	s^{-1}
力	ニュートン	N	m·kg/s^2
圧力，応力	パスカル	Pa	N/m^2
エネルギー,仕事,熱量	ジュール	J	N·m
工率，放射束	ワット	W	J/s
電気量，電荷	クーロン	C	A·s
電位，電圧，起電力	ボルト	V	W/A
静電容量	ファラド	F	C/V
電気抵抗	オーム	Ω	V/A
コンダクタンス	ジーメンス	S	A/V
磁束	ウェーバ	Wb	V·s
磁束密度	テスラ	T	Wb/m^2
インダクタンス	ヘンリー	H	Wb/A
セルシウス温度	セルシウス度	℃	
光束	ルーメン	lm	cd·sr
照度	ルクス	lx	lm/m^2
放射能	ベクレル	Bq	s^{-1}
吸収線量	グレイ	Gy	J/kg
線量等量	シーベルト	Sv	J/kg

表4　SIと共に暫定的に維持される単位

名称	記号
オングストローム	Å
バーン	b
バール	bar
ガル	Gal
キュリー	Ci
レントゲン	R
ラド	rad
レム	rem

1 Å=0.1nm=10^{-10}m

1 b=100fm^2=10^{-28}m^2

1 bar=0.1MPa=10^5Pa

1 Gal=1cm/s^2=10^{-2}m/s^2

1 Ci=3.7×10^{10}Bq

1 R=2.58×10^{-4}C/kg

1 rad=1cGy=10^{-2}Gy

1 rem=1cSv=10^{-2}Sv

表5　SI接頭語

倍数	接頭語	記号
10^{18}	エクサ	E
10^{15}	ペタ	P
10^{12}	テラ	T
10^{9}	ギガ	G
10^{6}	メガ	M
10^{3}	キロ	k
10^{2}	ヘクト	h
10^{1}	デカ	da
10^{-1}	デシ	d
10^{-2}	センチ	c
10^{-3}	ミリ	m
10^{-6}	マイクロ	μ
10^{-9}	ナノ	n
10^{-12}	ピコ	p
10^{-15}	フェムト	f
10^{-18}	アト	a

（注）

1．表1－5は「国際単位系」第5版，国際度量衡局 1985年刊行による。ただし,1 eVおよび1 uの値はCODATAの1986年推奨値によった。

2．表4には海里，ノット，アール，ヘクタールも含まれているが日常の単位なのでここでは省略した。

3．barは，JISでは流体の圧力を表わす場合に限り表2のカテゴリーに分類されている。

4．EC閣僚理事会指令ではbar，barnおよび「血圧の単位」mmHgを表2のカテゴリーに入れている。

換算表

力	N(=10^5dyn)	kgf	lbf
	1	0.101972	0.224809
	9.80665	1	2.20462
	4.44822	0.453592	1

粘度　1 Pa·s(N·s/m^2)=10 P(ポアズ)(g/(cm·s))

動粘度　1m^2/s=10^4St(ストークス)(cm^2/s)

圧力	MPa(=10bar)	kgf/cm^2	atm	mmHg(Torr)	lbf/in^2(psi)
	1	10.1972	9.86923	7.50062×10^3	145.038
	0.0980665	1	0.967841	735.559	14.2233
	0.101325	1.03323	1	760	14.6959
	1.33322×10^{-4}	1.35951×10^{-3}	1.31579×10^{-3}	1	1.93368×10^{-2}
	6.89476×10^{-3}	7.03070×10^{-2}	6.80460×10^{-2}	51.7149	1

エネルギー・仕事・熱量	J(=10^7 erg)	kgf·m	kW·h	cal(計量法)	Btu	ft·lbf	eV
	1	0.101972	2.77778×10^{-7}	0.238889	9.47813×10^{-4}	0.737562	6.24150×10^{18}
	9.80665	1	2.72407×10^{-6}	2.34270	9.29487×10^{-3}	7.23301	6.12082×10^{19}
	3.6×10^6	3.67098×10^5	1	8.59999×10^5	3412.13	2.65522×10^6	2.24694×10^{25}
	4.18605	0.426858	1.16279×10^{-6}	1	3.96759×10^{-3}	3.08747	2.61272×10^{19}
	1055.06	107.586	2.93072×10^{-4}	252.042	1	778.172	6.58515×10^{21}
	1.35582	0.138255	3.76616×10^{-7}	0.323890	1.28506×10^{-3}	1	8.46233×10^{18}
	1.60218×10^{-19}	1.63377×10^{-20}	4.45050×10^{-26}	3.82743×10^{-20}	1.51857×10^{-22}	1.18171×10^{-19}	1

1 cal= 4.18605J（計量法）

= 4.184J（熱化学）

= 4.1855J（15℃）

= 4.1868J（国際蒸気表）

仕事率　1 PS(仏馬力)

= 75 kgf·m/s

= 735.499W

放射能	Bq	Ci
	1	2.70270×10^{-11}
	3.7×10^{10}	1

吸収線量	Gy	rad
	1	100
	0.01	1

照射線量	C/kg	R
	1	3876
	2.58×10^{-4}	1

線量当量	Sv	rem
	1	100
	0.01	1

（86年12月26日現在）

Nuclear, Thermo-mechanical and Tritium Release Analysis of ITER Breeding Blanket